Advancing the Anaerobic Biofilm Membrane Bioreactor

by

Brian Aaron Roman

A Thesis Presented in Partial Fulfillment
of the Requirements for the Degree
Master of Science

Approved October 2021 by the
Graduate Supervisory Committee:

Bruce Rittmann, Chair
Joshua Boltz
Peter Fox
François Perreault

ARIZONA STATE UNIVERSITY

December 2021

ABSTRACT

The waterways in the United States are polluted by agricultural, mining, and industrial activities. Recovery of valuable materials, such as energy and nutrients, from these waste streams can improve the economic and environmental sustainability of wastewater treatment. A number of state-of-the-art anaerobic bioreactors have promise for intensified anaerobic biological treatment and energy recovery, but they have drawbacks. The drawbacks should be overcome with a novel anaerobic biological wastewater treatment process: the anaerobic biofilm membrane bioreactor (AnBfMBR). This research works aims to advance key components of the AnBfMBR.

The AnBfMBR is a hybrid suspended growth and biofilm reactor. The two main components of an AnBfMBR are plastic biofilm carriers and membranes. The plastic biofilm carriers provide the surface onto which the biofilms grow. Membranes provide liquid-solid separation, retention of suspended biomass, and a solids-free effluent. Introducing sufficient surface area promotes the biofilm accumulation of slow-growing methanogens that convert volatile fatty acids into methane gas. Biofilms growing on these surfaces will have a mixed culture that primarily consists of methanogens and inert particulate solids, but also includes some acetogens. Biomass that detaches from biofilms become a component of the suspended growth. A bench-scale AnBfMBR was designed by the AnBfMBR project team and constructed by SafBon Water Technology (SWT).

The primary objective of this thesis project was to evaluate the ability of plastic biofilm carriers to minimize ceramic-membrane fouling in the AnBfMBR setting. A systematic analysis of mixing for the bench-scale AnBfMBR was also conducted with the

plastic biofilm carriers. Experiments were conducted following a 'run to failure' method, in which the ceramic membranes provide filtration, and the time it takes to reach a 'failure transmembrane pressure (TMP)' was recorded.

The experiments revealed two distinct trends. First, the time to failure TMP decreased as mixed liquor suspended solids concentration (MLSS) concentration increased. Second, increasing the carrier fill extend the time to failure, particularly for higher MLSS concentrations. Taken together, the experiments identified an optimized "sweet spot" for the AnBfMBR: an operating flux of 0.25-m/d, a failure TMP of 0.3-atm pressure, MLSS of 5,000 – 7,500 mg/L, and 40% carrier fill.

AWKNOWLEDGEMENTS

This thesis is dedicated to my family for their unconditional love and support, especially during my Undergraduate and Master's studies at Arizona State University (ASU). Going to a university so far away from home was difficult, but my family's unwavering support enabled me to thrive and pursue my dreams. I am thankful for my entire family, especially to my parents, little siblings, and grandparents. I am also thankful for my family in New Mexico, who have been an incredible support system for me during my time at ASU.

I consider myself extremely fortunate to have had the opportunity to work with Drs. Bruce Rittmann and Josh Boltz during my graduate studies at ASU. Dr. Rittmann is a true inspiration, and I am grateful for his assistance not only with my research, but also with navigating the PhD application process in order to continue my graduate school pursuits. I am grateful to Dr. Boltz for his constant encouragement, enthusiasm for my research progress, and eagerness to assist in my professional development. Dr. Rittmann and Dr. Boltz have become true role models for me, and I will miss them greatly during my doctoral program at the University of Washington.

This project would not have been possible without financial funding by PepsiCo along with the Swette Center for Environmental Biotechnology (SCEB) at ASU. I am grateful to everyone at SCEB for their friendliness and constant willingness to assist me my research. I specifically want to thank Yuhang Cai, Michelle Young, Carole Flores, Chris Muse, and Sarah Arrowsmith. I also am thankful to Dr. Peter Fox and François Perreault, who serve on my committee.

TABLE OF CONTENTS

Page

CHAPTER Page

APPENDIX Page

LIST OF TABLES

Table Page

LIST OF FIGURES

Figure Page

1 Introduction

1.1 Sustainable Wastewater Treatment

Many waterways in the United States of America (USA) are polluted by agricultural, mining, and industrial activities. Microbiological treatment is a proven process to lessen pollutant inputs to waterways. A specifically good application is the treatment of wastewater with a high concentration of organic matter, because anaerobic biological treatment can eliminate pollutant discharge while also recovering energy, nutrients, and other valuable materials from the waste streams (Hao, Van Loosdrecht, Jiang, and Liu, 2019). Recovery of valuable materials can improve the economic and environmental sustainability of wastewater treatment.

1.2 Aerobic vs Anaerobic Wastewater Treatment

A key distinction for microbiological treatment technologies is whether they are aerobic or anaerobic, such as activated sludge versus various anaerobic processes (Rittmann and McCarty, 2001). Aerobic treatment occurs in the presence of oxygen, an electron acceptor that must be supplied and incurs significant energy and economic costs (Rittmann and McCarty, 2020). In contrast, anaerobic treatment excludes oxygen, which eliminates the cost of its delivery, while opening up the option to generate and recover methane gas.

The most widely used aerobic biological process is activated sludge, which commonly consists of an aeration tank, a settling tank, solids recycle, and sludge wasting (Rittmann and McCarty, 2020). **Figure 1** is a schematic of traditional activated sludge. The sludge is "activated" by accumulating a high concentration of biomass through sludge settling and recycling (Rittmann and McCarty, 2020). The aeration tank is a

suspended-growth reactor containing microbial aggregates of microorganisms that consume and oxidize input organic electron donors (i.e., the biochemical oxygen demand, or BOD). The mixed liquor, which is the suspension containing the microbial aggregates, passes to the settling tank, where the aggregates are removed from the treated wastewater by settling and either returned to the aeration tank or wasted. Sludge is wasted to control the solids retention time (SRT), which is the fundamental design parameter to control the performance of an activated sludge process. SRT is inversely proportional to the specific growth rate of the active microorganisms, which controls the concentration of the growth-rate-limiting substrate in the reactor (Rittmann and McCarty, 2020).

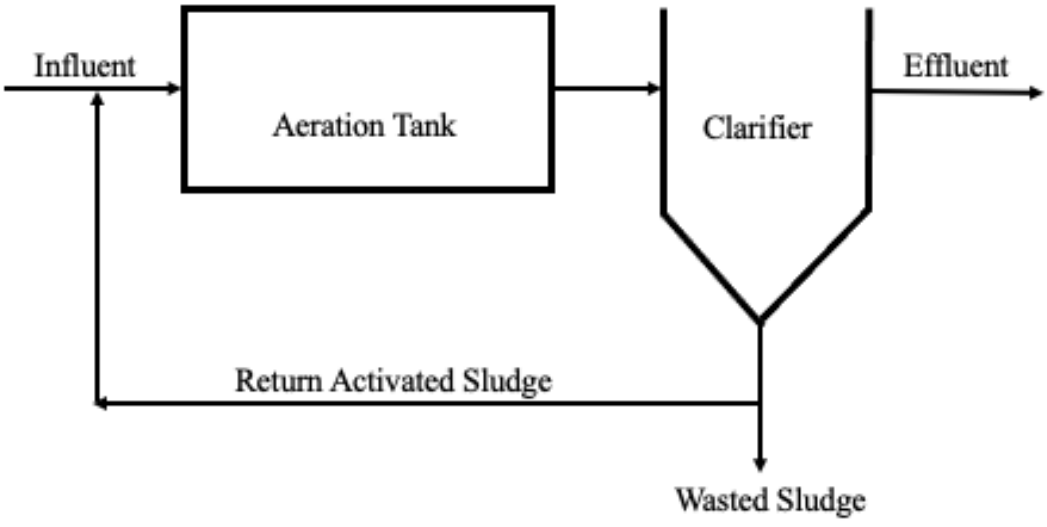

Figure 1. Schematic of the traditional activated sludge process.

The activated sludge process can be intensified, or operated with a higher volumetric loading, by modifying it to an Aerobic Membrane BioReactor (AeMBR). **Figure 2** is a schematic of the two most common configurations of an AeMBR. The

AeMBR combines activated sludge technology with membrane filtration to expand the normal operating range of mixed liquor suspend solids (MLSS) concentrations. Membranes provide better and more stable effluent quality, as the effluent is devoid of any suspended solids. AeMBRs intensify the process because they can be designed for MLSS concentrations, because they are not affected by the limitations of gravity sedimentation for liquid-solid separation.

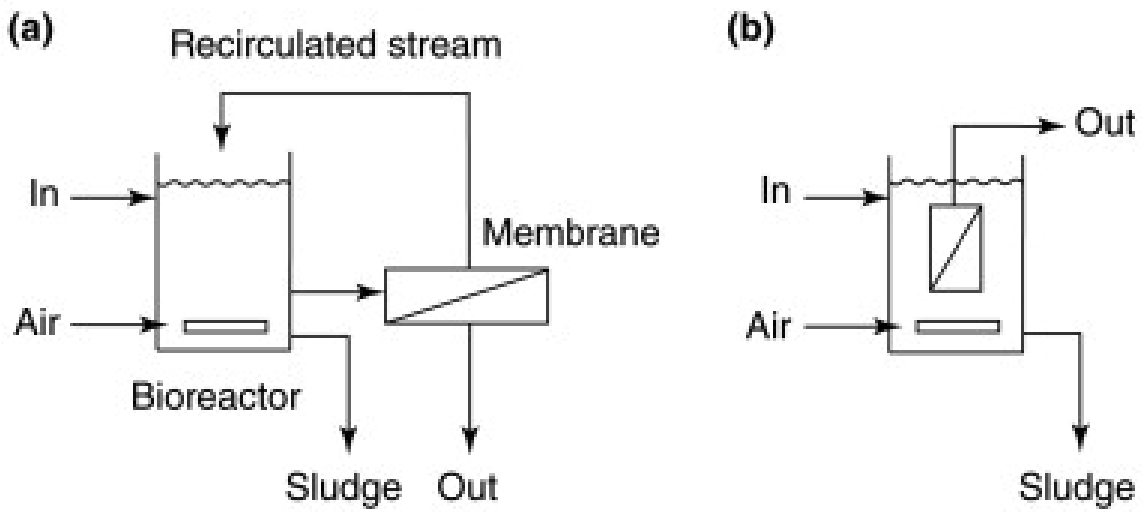

Figure 2. Schematic of the traditional Aerobic Membrane BioReactor process; (a) side-stream (b) immersed. Source: Judd (2008)

Anaerobic treatment excludes all oxygen gas (O_2), which allows a strictly anaerobic microbial community to develop. The key is that the input organic matter is ultimately stabilized to form methane gas (CH_4), which evolves from the water. Anaerobic biological wastewater treatment provides many advantages compared to aerobic treatment. The main advantages stem from the absence of aeration. Aeration is an energy-intensive process; eliminating it in anaerobic treatment makes the process more energy sustainable and cost-effective than aerobic wastewater treatment. Additionally, the absence of aeration eliminates the prime limitation on volumetric

loading in activated sludge: the volumetric rate of O_2 supply. From a capital-cost standpoint, anaerobic wastewater treatment can be designed to sustain a greater volumetric loading rate than aerobic wastewater treatment; therefore, it can have a smaller tank volume and less capital expense. Finally, anaerobic wastewater treatment produces energy in the form of methane gas, which can make anaerobic treatment a net energy producer.

A widely used anaerobic biological process is anaerobic digestion, which converts complex organic solids into methane, reducing the mass organic solids and the pathogen content of the sludge (Parkin and Owen, 1986). Anaerobic microbiology is complex and requires many different types of microorganisms that have syntrophic relationships (Rittmann and McCarty, 2001). **Figure 3** illustrates microbiological steps of anaerobic digestion, which is used to treat sludges and other organic streams that have high concentrations of organic solids. The four major processes are hydrolysis, acidogenesis, acetogenesis, and methanogenesis. The first step is hydrolysis, which breaks down complex solids and polymers to soluble forms. Second is acidogenesis, which forms fatty acids. Third is acetogenesis, which breaks down the fatty acids to acetic acid, H_2 and CO_2. Lastly is methanogenesis, which converts acetic acid and H_2 methane (Rittmann and McCarty, 2020).

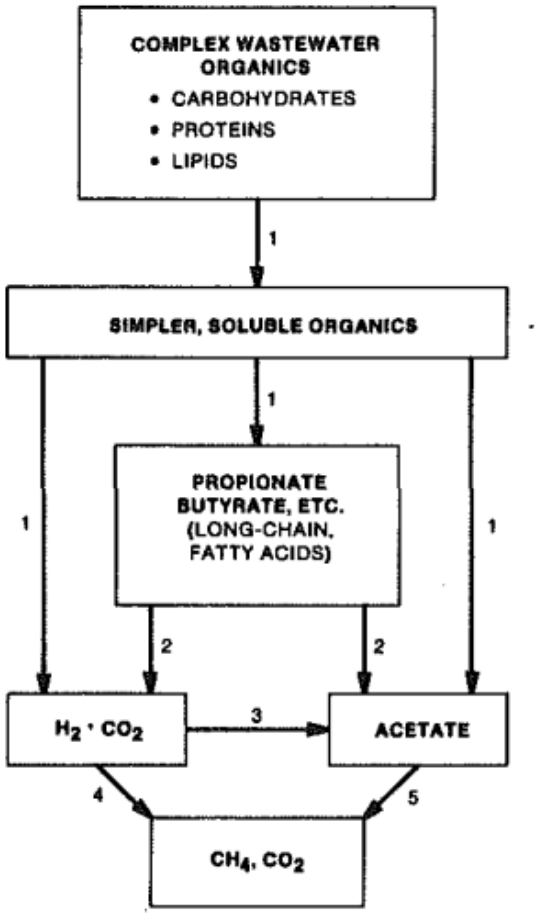

Figure 3. Steps leading to methane formation in anaerobic digestion. Source: Parkin and Owen (1986)

Key factors for efficient digestion include providing adequate contact between the bacteria and their food sources and sufficient microbial retention time, or SRT (Parkin and Owen, 1986). One of the biggest shortcomings of traditional anaerobic digestion is that the SRT equals the hydraulic retention time (HRT). This condition is not feasible for wastewater treatment, as the reactor volume and size will be too large, directly affecting capital costs and land-area requirements. Another drawback of traditional anaerobic digestion is the poor effluent quality. The supernatant from treated sludge thickening and dewatering contains substantial suspended solids, dissolved and particulate organic

materials, ammonia nitrogen, and phosphorus (Dohányos, Zabranksa, Kutil, and Jeníček, 2004).

The leading technology for intensifying anaerobic treatment while also improving its effluent quality is the Anaerobic Membrane BioReactor (AnMBR), and a few commercial options are available. **Figure 4** presents a simple flow diagram of a submerged AnMBR, which has a membrane module immersed in a bioreactor, a permeate pump, and biogas that is delivered to the bioreactor at the base of the membranes.

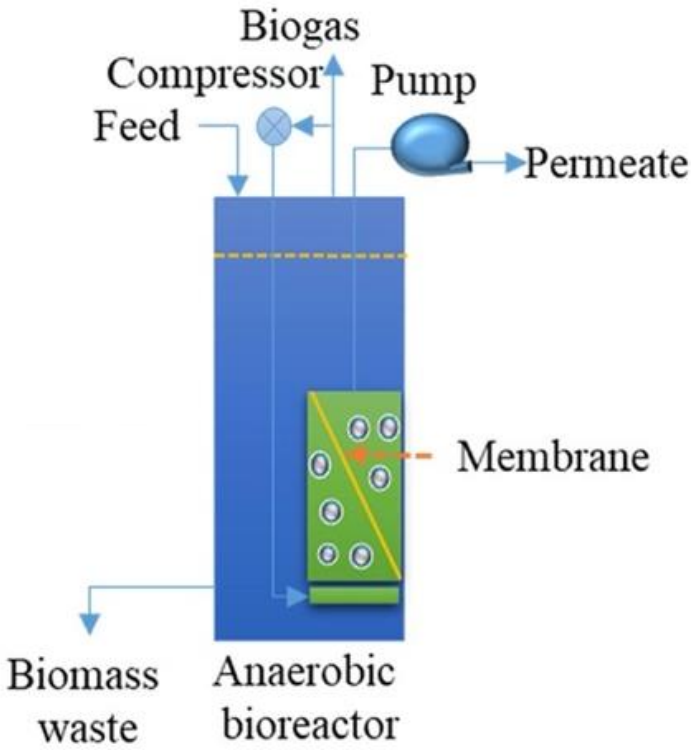

Figure 4. Configurations of a submerged Anaerobic Membrane Bioreactor. Source: Maaz et al., (2019).

Figure 5 is a flow diagram for a commercially available AnMBR process marketed by Suez Water Technologies and Solutions. The Suez AnMBR has a feed

pump, single-stage reactor, effluent from the bioreactor that flows into a separate stage membrane tank, which uses hollow fiber polymeric membranes, a recirculation stream that is directed back to the bioreactor, headspace gas is extraction and storage, and permeate pumped for use or subsequent treatment.

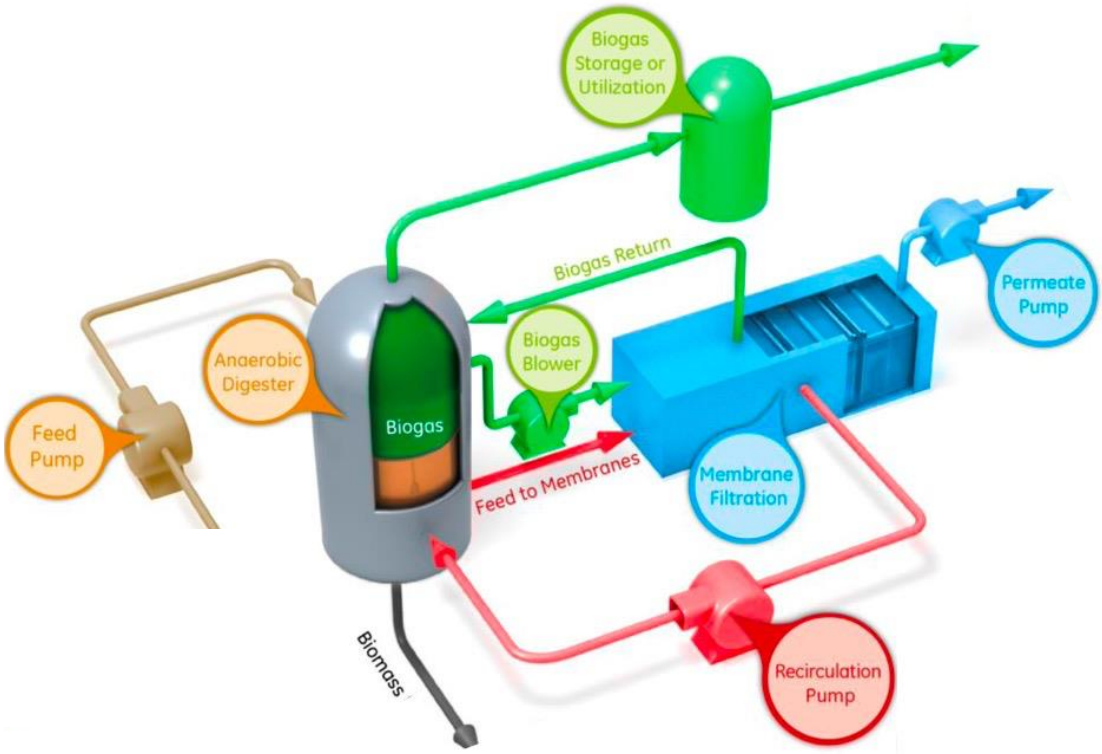

Figure 5. Flow diagram of the AnMBR marketed by Suez Water Technologies and Solutions (France). Source: Suez Water Technologies and Solutions (2021)

One of the drawbacks of the Suez technology is the separate-stage membrane tank. According to Smith et al. (2014), a sustainable permeate flux across the membrane surfaces is 0.25 $m^3/d.m^2$. This value is based on pilot-scale investigations using hollow fiber polyvinylidene membranes. The pumping of mixed liquor to and from the separate membrane tank adds significant energy cost. Furthermore, the gas flow required for membrane sparging flux is ~2 $m^3/d.m^2$ (Smith et al., 2014). This value results in a high

sparging time (~25% of operation time), which is a significant energy demand and requires the use extra membranes. Another drawback is the use of polymeric membranes, which may have a short operating life.

An alternative to the AnMBR is the Anaerobic Granular Sludge (AnGS) process. **Figure 6** presents an example of an AnGS, developed by PAQUES. The PAQUES technology has a feed pump, anaerobic granular sludge in an expanded bed reactor, pumps for internal recycle, and gas extraction and storage. The downfall with this technology is that it requires separate-stage liquid solid separation. Therefore, it will require additional footprint and additional energy.

Figure 6. Anaerobic Granular Sludge (PAQUES, The Netherlands). Source: PAQUES (2021).

An emerging anaerobic technology is the Anaerobic Moving Bed Bioreactor (AnMBBR) by Veolia, shown in **Figure 7.** The AnMBBR requires a feed pump,

mechanical mixers, plastic biofilm carriers, screen walls, and gas extraction and storage. The AnMBBR, like the AnGS, has no liquid-solid separation and requires a separate unit.

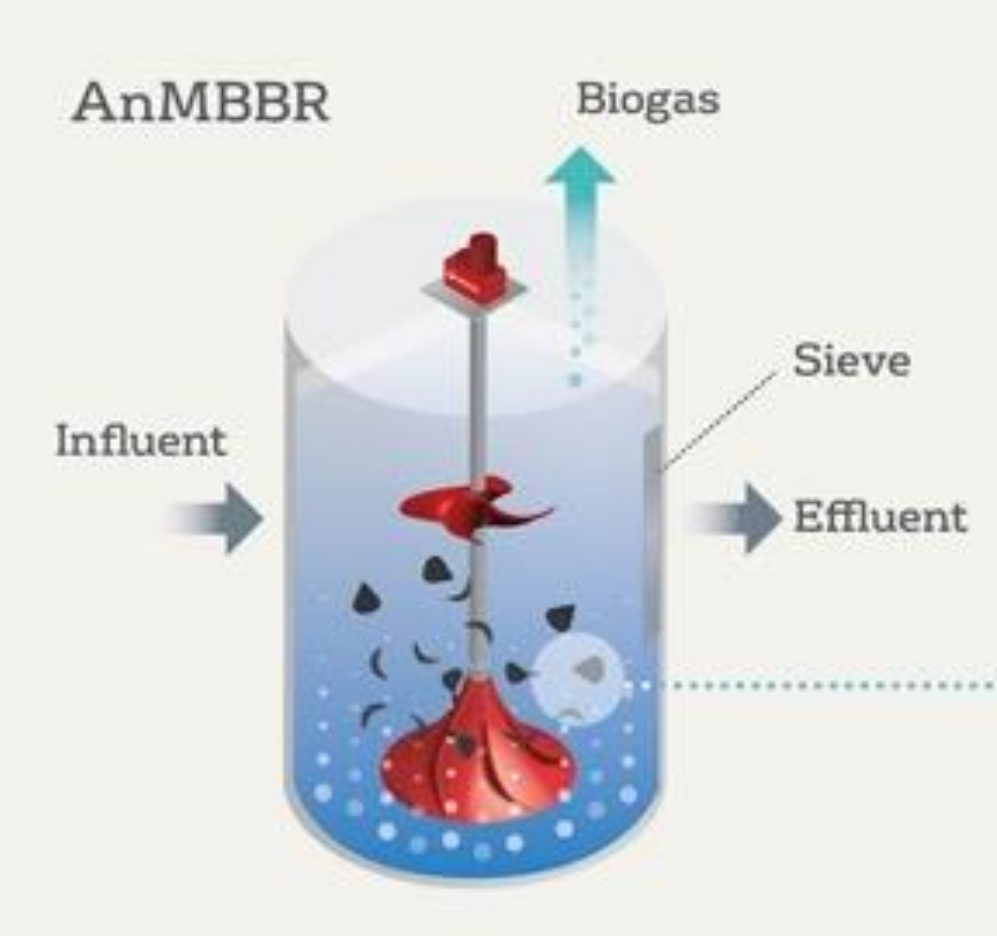

Figure 7. Anaerobic Moving Bed Bioreactor (Veolia, France). Source: Biothane Solutions (2021)

In summary, anaerobic biological treatment has advantages over activated sludge: methane production instead of oxygen delivery and a higher volumetric loading. Three state-of-the-art anaerobic bioreactors for treating wastewater (AnMBR, AnGS, AnMBBR) have promise for intensified anaerobic biological treatment, but they have drawbacks. The AnMBBR and AnGSR have relatively poor effluent water quality because of particulate chemical oxygen demand (PCOD) in the treated effluent. These

two technologies also require a separate-stage liquid-solid separation. While AnMBRs have effective liquid-solid separation, frequent membrane backwashing requires significant energy.

The work in this thesis is based on an understanding that AnMBRs are the best technology base, but they can be improved upon. The Water Environment Federation's Manual of Practice 8, namely *Design of Water Resource Recovery Facilities*, offer strong support of this point-of-view:

> "In order to make full-scale AnMBR installations a reality, future research needs to focus on less-energy-intensive membrane fouling prevention techniques and methods of removing dissolved methane in the permeate at low temperatures (Smith et al. 2013). Similar to aerobic MBR treatment, many AnMBR studies have used backflushing and biogas sparging, which have been successful in preventing membrane fouling; however, (they) are highly energy intensive."

All of these drawbacks should be overcome with a novel anaerobic biological wastewater treatment process: the anaerobic biofilm membrane bioreactor (AnBfMBR). This research works aims to advance key components of the AnBfMBR.

1.3 Introduction to and Advantages of the AnBfMBR

The AnBfMBR is a hybrid bioreactor that accumulates acidogens/acetogens primarily in its suspended solid and methanogens primarily its biofilm. Introducing an adequate surface area promotes the biofilm accumulation of methanogens that are capable of converting most of the VFA into methane. Biofilms growing on these surfaces will have a mixed culture that primarily consists of methanogens and inert particulate chemical

oxygen demand (COD), but also includes some acetogens. Biomass that detaches from biofilms become a component of the suspended growth.

The first key component of the AnBfMBR is a plastic biofilm carrier. Biological treatment of wastewaters can be achieved with suspended growth, biofilms, or both together. Suspended growth involves bacterial aggregates/flocs that are suspended in the bulk of a liquid. Biofilms are microbial aggregates attached to a solid surface. Attachment is the means to retain the biomass without the need of a settler or a filter. Substantial environmental and monetary benefit may be associated with processes conceptualized and designed to promote and utilize suspended growth and biofilm interactions (Aqeel, Weissbrodt, Cerruti, Wolfaardt, Wilen, and Liss, 2019). A fundamental basis of these hybrid processes is the separation of bacterial compartments (i.e., into suspended growth and biofilm) by the rate at which targeted bacteria can biologically transform substrates in wastewater. In this case, the targeted microorganisms include methanogens and acetogens, which work in tandem to anaerobically transform organic pollutants into methane.

Mobile biofilm carriers may be organic in nature (e.g., kenaf particles) or man-made materials (e.g., high density polypropylene). The two plastic carriers used in this research were provided by Veolia Water Technologies: K5 and Z carriers, with the characteristics listed in **Table 1** and **Table 2**, respectively. Photographs of these plastic carriers are shown in **Figure 8** and **Figure 9**. These carriers were designed to provide a repeatable surface area that promotes the accumulation biofilm. The K-5 carriers are shaped like small cylinders and its high degree of surface area help aid in the formation of biofilms. The Z carriers are fabricated with a plastic grid that has a 200-µm depth (i.e.,

Z-200) or a 400-µm depth (Z-400). In principle, a Z-200 carrier can accumulate a biofilm with a maximum thickness of 200 µm, while a Z-400 plastic carrier can accumulate a maximum thickness of 400 µm.

Table 1. Veolia-reported biofilm-carrier characteristics

Name	**Bulk Specific Surface Area**	**Maximum Carrier Fill in a Bioreactor**	**Nominal Carrier Thickness; Diameter**
K5	800 m_F^2/m_C^3	60%	4 mm; 25 mm
Z-Carrier	1,500 m_F^2/mp	0.20 mp/m_R^3 (anaerobic MBBR) 0.24 mp/m_R^3 (aerobic MBBR)	10 mm (equivalent); 30 mm (approximate)

Table 2. Veolia-reported Z-carrier characteristics

Type of Z-Carrier	**Grid Depth (µm)**	**Mass (kg/m_C^3)**
Z-200	200	210
Z-400	400	263

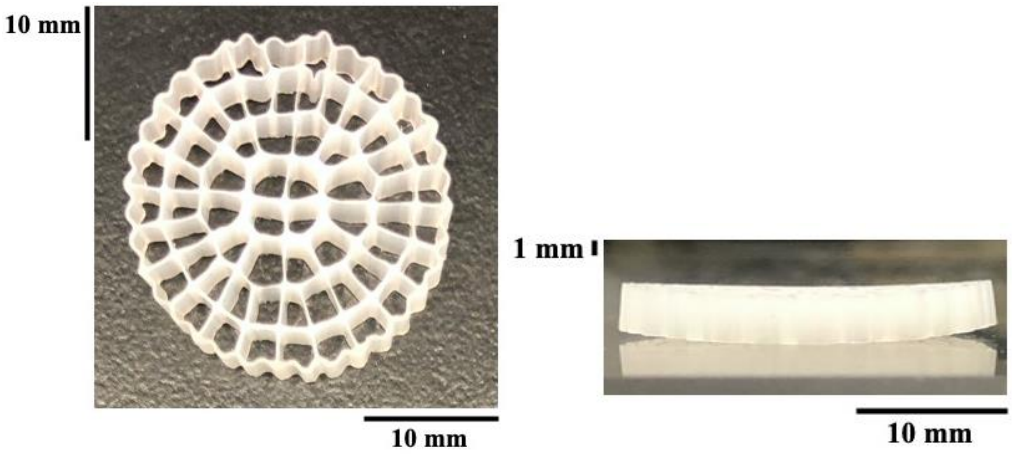

Figure 8. Plan and Profile View of K5 carriers

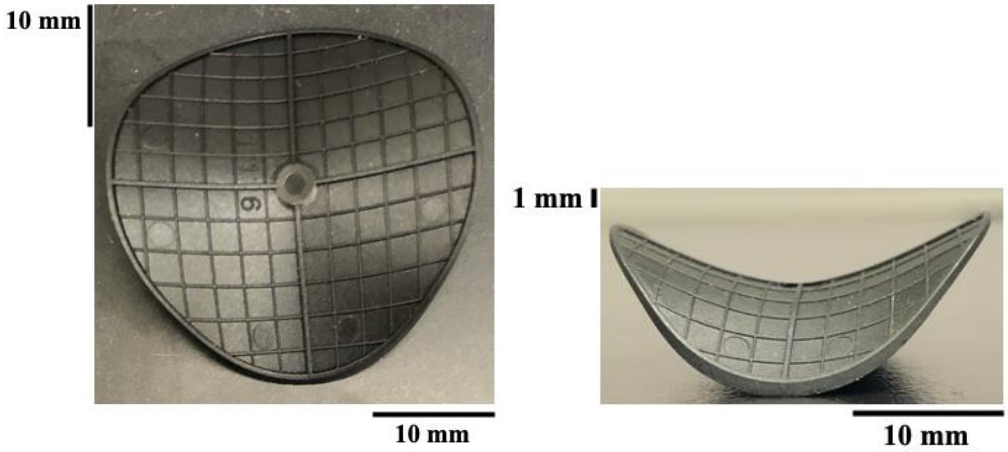

Figure 9. Plan and Profile View of a Z-400 Carrier. The 400–µm grid is clearly evident.

Another key component of the AnBfMBR is a membrane, which provides the liquid-solid separation and solids-free effluent. The type of membranes used in an AnBfMBR are ceramic membranes, which exist as plates that are collected in modules. A standard ceramic membrane module is shown in **Figure 10** (SafBon Water Technology, U.S.A.). Ceramic membranes are preferred over polymeric membranes because of their durability, particularly when plastic carriers are present. Advantages of ceramic membranes over polymeric membranes include higher flux (due to less fouling), longer lifespan, and more mechanical, thermal, and chemical stability (Gitis and

Rothenburg, 2016). For example, ceramic membranes manufactured by SafBon Water Technology may have up to 5-fold longer lifespan, up to 2 times higher flux rates, up to 50% less chemicals required for cleaning interventions, and up to 50% lower personnel costs for operation and maintenance, compared to polymeric membranes (SafBon Water Technology, U.S.A.). Currently, ceramic membranes are more expensive than polymeric membranes, because ceramic membranes require more costly materials and have a more complex fabrication process (Gitis and Rothenburg, 2016). However, their advantages in the context of the AnBfMBR may take precedence.

Figure 10. SafBon Water Technology Ceramic Membrane Standard Module. Source: SafBon Water (2021).

The AnBfMBR has several potential advantages over the AnMBR. According to Smith et al. (2012), membrane fouling continues to be a primary challenge to implementing any MBR system, aerobic or anaerobic, because of its direct effect on capital and operating costs. In an AnBfMBR, the interaction between plastic carriers and ceramic membranes helps to address and allay this longstanding concern about

membrane bioreactors. In an AnBfMBR, the plastic carriers continuously scour membrane surfaces. A few number studies have explored this interaction. Jin, Ong, and Ng (2013) conducted a study on two identical submerged ceramic membrane bioreactors (SCMBRs) – one with carriers (AnoxKaldnes, K1 carrier) and one without – to investigate membrane fouling control mechanisms associated with plastic carriers. The results indicated that carriers were capable of delaying fouling because the carriers helped to shear off cake that was formed on the membrane (Jin et al., 2013). Guo, Guan, and Xia (2014) conducted a similar study and observed that carriers scrubbed the membrane and extended operating time of a submerged membrane bioreactor. Closely related is the effect of plastic carriers on trans-membrane pressure (TMP), which is correlated to membrane fouling. Guo et al. (2014) concluded that TMP increased in the reactor with plastic carriers were slower than the reactor without, because the carriers minimized the membrane fouling.

Another well-studied and successful example is the staged anaerobic fluidized membrane bioreactor (SAF-MBR), shown in **Figure 11** (Kim, Kim, Ye, Lee, Shin, McCarty, and Bae, 2011). The first stage is an anaerobic fluidized bed in which the fluidized carrier is granular activated carbon (GAC). GAC is lightweight and has many macropores that are effective for harboring slow-growing methanogens. Then, the effluent from the first stage goes to the second stage, which is also a GAC-based fluidized bed. GAC is immersed into the second reactor as a natural cleaning mechanism of membranes to reduce biofouling. Although the performance of the SAF-MBR was excellent in terms of effluent quality and low TMP, pilot studies in the United States and South Korea showed that the constant contact of GAC carriers against the hollow-fiber

membranes damaged the membranes (Kim et al., 2011). This finding was a prime motivation for our decision to utilize ceramic membranes. Furthermore, other biofilm carriers are possible, and this thesis explores the effectiveness of the K5 and Z carriers provided by Veolia Water Technologies.

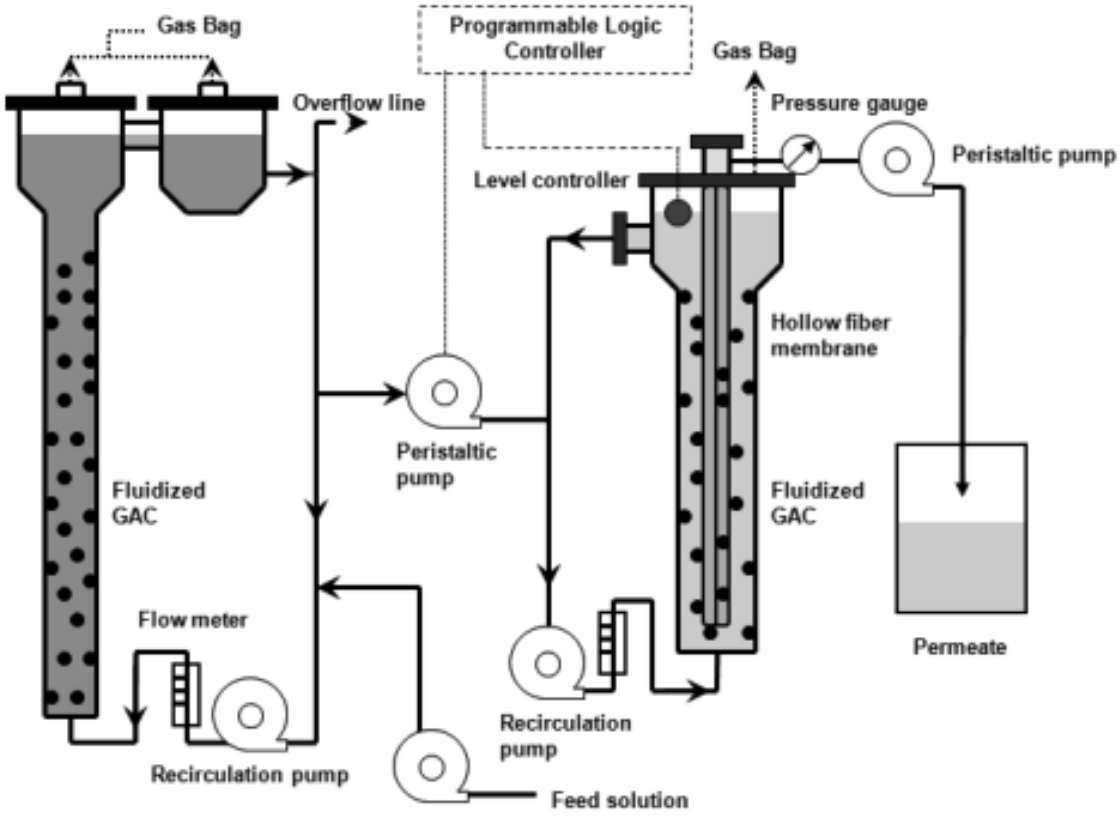

Figure 11. Staged anaerobic fluidized membrane bioreactor (SAF-MBR). Source: Kim et al. (2011)

1.4 Objectives

The primary objective of this thesis is to evaluate the ability of plastic biofilm carriers to minimize ceramic-membrane fouling in the AnBfMBR setting. Specific objectives include: 1) an evaluation of essential, but so-far unreported characteristics of K5 and Z carriers; 2) a systematic evaluation of how MLSS controls permeate flux with ceramic membranes; 3) documentation of the impact of biofilm carriers on mitigating

membrane fouling and TMP buildup for a relevant range of MLSS concentrations and carrier-fill ratios; and 4) evaluation of the impact of power input values on biofilm carrier membrane mixing and scouring efficiency.

The thesis is organized into the following chapters:

- Chapter 2 reviews the experimental design and operation of a bench-scale AnBfMBR. This chapter also includes a mixing analysis for the bench-scale AnBfMBR.
- Chapter 3 details the physical characteristics of the plastic biofilm carriers.
- Chapter 4 examines the results of the experiments on the effects of MLSS, carrier fill, and mixing power on the buildup of TMP in the bench-scale AnBfMBR.
- Chapter 5 summarizes the thesis and makes recommendations for future study into the AnBfMBR.

2 Methods and Materials

2.1 Reactor Feed

Anaerobic digestor (AD) sludge samples were retrieved from the City of Mesa Northwest Water Reclamation Facility (NWWRP) at the beginning of each week, usually on Monday or Tuesday. AD sludge was sampled from the bottom of the anaerobic digesters using a sampling valve in the sludge recirculation line. A total of 40-L of AD sludge was sampled for each visit at the NWWRP. All samples were transported to the Biodesign Swette Center for Environmental Biotechnology (BSCEB) and stored in a general use fume hood for a maximum of five days before use.

Five mixed liquor suspended solids (MLSS) concentrations were tested: 1, 3, 5, 7.5, and 10 g/L. The biomass from the AD sludge was diluted with tap water to reach the desired MLSS concentration. **Equation 1** defines the volume of AD sludge used in an experiment.

$$V_{Sludge} = \frac{C_{Sludge,Desired} V_{Reactor}}{C_{Sludge,Actual}} \quad (1)$$

where

V_{Sludge} = volume of AD sludge, L

$V_{Reactor}$ = volume of bench-scale reactor, L

$C_{Sludge,Desired}$ = desired MLSS concentration, g/L

$C_{Sludge,Actual}$ = measured MLSS concentration of AD sludge, g/L

Equation 2 defines the volume of tap water added into the bench-scale reactor to reach $C_{sludge,Desired}$.

$$V_{Water} = V_{Reactor} - V_{Sludge} \quad (2)$$

where

V_{Water} = volume of tap water added to the bench-scale reactor, L

2.2 Analytical Methods

Two tests were performed according to *Standard Methods* (1998): total suspended solids (TSS) and volatile suspended solids (VSS). Procedures are described briefly below. TSS and VSS were determined by filtering a 2-mL volume through a 1.2-μm glass microfiber filter using a vacuum filter apparatus. All samples are assayed in triplicate. Prior to filtering a sample, the filter mass was recorded (W_1) for each sample. Filters with collected solids were dried in a 105°C oven for approximately 24 hours. Filters were then transferred to a desiccator box for three hours. The mass of the dried filter was then recorded (W_2). Filters were transferred to a 550°C oven for 30 minutes and then immediately transferred to a desiccator box for 10 minutes. The mass of the dried filter was then recorded (W_3). TSS and VSS were computed from **Equations 3** and **4**.

$$TSS\ (g/L) = \left(\frac{W_2 - W_1}{2\ mL}\right) \cdot \frac{1{,}000\ mL}{L} \quad (3)$$

$$VSS(g/L) = \left(\frac{W_2 - W_3}{2\ mL}\right) \cdot \frac{1{,}000\ mL}{L} \quad (4)$$

Measurements for TSS and VSS are conducted for every new batch of AD sludge samples from the NWWRP.

2.3 Bench-Scale Anaerobic Biofilm Membrane Bioreactor

A bench-scale AnBfMBR was designed by the Arizona State University (ASU) AnBfMBR project team and constructed by SafBon Water Technology (SWT). **Figure 12** depicts the bench-scale AnBfMBR used in the experiments. **Table 3** lists the key equipment and instrumentation for the bench-scale AnBfMBR.

Figure 12. Photograph of the bench-scale AnBfMBR

Table 3. Equipment and Instrumentation List for the Bench-Scale AnBfMBR

Item	Description
Tank	Material: Acrylic Plexiglass Capacity: 110 L Dimensions: 28”(L) x 13”(W) x 18” (H)
Membrane	Material: α-Al_2O_3 (Aluminum Oxide) Pore size: 0.2 μm Membrane Area: 0.18 m^2 Membrane Plate Dimensions: 400mm(L) x 175mm (W) x 140mm (H) Membrane Plate Spacing: 65-mm
Mixing Pump	Type: Centrifugal Pump, 0.5 HP, 3450 RPM
Permeate/Backwash Pump	Type: Peristaltic Pump
Mixing System	Four Orifice Jets
Flow Transmitter (1)	Use: Influent Flow
Flow Transmitter (2)	Use: Permeate Flow
Pressure Transmitter	Use: Permeate Flow
Piping/Tubing	Polypropylene tubing with quick connect fittings

2.4 Bench-Scale Anaerobic Biofilm Membrane Bioreactor Mixing System Analysis

Ideally, plastic biofilm carriers are homogeneously distributed in the bulk liquid of an AnBfMBR, but the plastic biofilm carriers are buoyant and tend to accumulate near the water surface. Therefore, a mixing-system was used to distribute the plastic biofilm carriers and suspended solids in the AnBfMBR. The plastic biofilm carriers provide surfaces for biofilm growth and control membrane biofouling through interactions with ceramic ultrafiltration (UF) membranes surfaces. These interactions are controlled through mixing-energy input, bulk-liquid mixing pattern, spacing in between ceramic UF membrane plates surfaces, and ceramic UF membranes location inside an AnBfMBR. Proper mixing-system design is critical for AnBfMBR scale up and minimizing mixing-energy requirements, capital expenses, and equipment damage. However, much is unknown about plastic biofilm carriers mixing-system design. Commonly, mechanical

mixers are used in anaerobic moving-bed biofilm reactors (MBBR) (McQuarrie and Boltz, 2011), and manually controlled valves in air pipes that unevenly distribute air-flow and promote a rolling water-circulation pattern in aerobic MBBR (Daigger and Boltz, 2018).

Typically, MBBR mixing is accomplished by rail-mounted mechanical mixers that are submerged in a bioreactor, or a mechanical mixer with a platform-mounted and non-submerged motor, vertically oriented shaft, and impeller. A company named INVENT manufactures non-submersible mixers that are platform-mounted, have a vertical shaft, and a hyperboloid-shaped mixer body. McQuarrie and Boltz (2011) suggested a 25-W/m^3 power input for submerged mechanical mixers in an anaerobic MBBR. It is important to note that having a mixer submerged or not should not affect the power inputs to the water. However, as described above, some mechanical mixers have submerged motors and others mount motors on a platform that is not submerged. The 25-W/m^3 power input is considered a maximum value that reliably and evenly distributes plastic biofilm carriers throughout a tank without damaging the mixing device or plastic biofilm carriers. It is desirable to control mechanical-mixing device motors using variable-frequency drives (VFDs), which allows an operator to optimize mixing-power input. An operator can reduce impeller speed to minimize energy required for mixing. Usually, 10- to 15-W/m^3 mixing-power inputs do not diminish process performance (e.g., effluent water quality).

Scalability and cost effectiveness are two important characteristics of a mixing system. The desire to progress from bench- to pilot-scale, and then from pilot- to full-scale, makes a scalable value essential for this research. Cost effectiveness is also an important consideration. Energy must be put into the system that is on par with the amount of methane being produced and its energetic value; the goal is to have a system be net

energy positive. Furthermore, plastic biofilm carriers should be well mixed without damaging them, the mechanical mixers, or the ceramic UF membranes. Therefore, the goal is to find the minimum power-input for mixing plastic biofilm carriers to achieve membrane biofouling control.

We anticipate that mechanical mixers will be a reliable and cost-effective mixing option for AnBfMBR's larger than bench-scale. However, the bench-scale experiments in this research effort do not use mechanical mixers because they are not amenable to use with our (bench-scale) experimental apparatus.

A hydraulic mixing system was used in this study. It has a pump, pipe network, and four orifice jets. Water in the bench-scale AnBfMBR was recycled. **Figure 13** depicts the bench-scale AnBfMBR mixing-system. **Figure 14** and **Figure 15** are sketches of the mixing-system. Mixing-system design and analysis are described in the following.

Figure 13. Bench-Scale AnBfMBR Mixing-System Components

Figure 14. Plan View of Bench-Scale AnBfMBR Mixing-System

Figure 15. Profile View of Bench-Scale AnBfMBR Mixing-System

2.4.1 Power Input Calculations

Power input and velocity gradient are useful for characterizing mixing systems. **Equation 5** defines power that can be gained by a fluid.

$$P = \gamma \cdot Q \cdot H \quad (5)$$

where

P = power, W

γ = specific weight of fluid, N/m^3

Q = volumetric flow rate, m^3/s

H = head, m

Equation 6 defines the velocity gradient, which is a fundamental parameter used to describe flocculation (Grady, Daigger, and Lim, 1999).

$$G = \sqrt{P / \mu \cdot V} \quad (6)$$

where

G = velocity gradient, 1/s

μ = dynamic viscosity, $N\text{-}s/m^2$

V = volume, m^3

With one exception, all variables in **Equation 5** and **Equation 6** are defined by the system specifications. The unspecified parameter is the total system head, defined in **Equation 7**.

$$\text{Total System Head} = \text{Static Head} + \text{Dynamic Head} \quad (7)$$

The first component of the head loss equation defined in **Equation 7** is static head loss. This is the difference between the water surface and pump discharge. For the bench-scale AnBfMBR,

Static Head = 0.88 ft = 0.27 m

The second component of head loss is dynamic head, which consists of two parts: major head losses and minor head losses. It is also important to note that major head losses and minor head losses have two parts, because some pipes and fittings take the total flow, while some only require 1/4th of the total flow. For example, total flow had 4 90-degree elbows and one ball valve, while for 1/4th of total flow had two 90-degree bends and 2 standard tees.

Major head losses are predicted with the Colebrook-White Equation, defined in **Equation 8**.

$$\frac{1}{\sqrt{f}} = -2.0 \cdot \log_{10}\left(\frac{\frac{\varepsilon}{D}}{3.7} + \frac{2.51}{Re \cdot \sqrt{f}}\right) \quad (8)$$

where

f = friction factor

ε = relative roughness

D = pipe diameter, ft

Re = Reynolds Number

The Reynolds Number is defined in **Equation 9**.

$$Re = \frac{\rho v D}{\mu} \quad (9)$$

where,

ρ = density of water, kg/m^3

v = average velocity, m/s

Reynolds Number is a dimensionless quantity associated with the smoothness of flow of a fluid relative to the energy absorbed within the fluid as it moves (Milnes, n.d.).

A low Reynolds number (Re ≤ 2000) means that viscous forces are dominant, and a high Reynolds Number (Re ≥ 3000) means that kinetic forces are dominant (Elger, LeBret, Crow, and Roberson, 2020).

The Colebrook-White Equation is an empirical equation that was developed by acquiring data for commercial pipes. It is used to estimate the friction factor. Because the Colebrook-White Equation cannot be solved in closed form, a trial-and-error method must be performed untile the left-hand side (LHS) and right-hand side (RHS) of the equation agree. I set up a Microsoft Excel spreadsheet to solve this equation. **Tables 4** and **5** summarize the results for the full flow rate of 12.5 GPM (0.0008 m^3/s) and 25% of the full flow rate, respectively. Calculations for other flow rates are presented in **Appendix A**, **Appendix B**, and **Appendix C.** The flow rates were chosen from a systematic mixing-analysis of K5 media and Z-400 carriers which is discussed later in this section.

First, an initial guess is input into the spreadsheet for the friction factor. Then, the solver tool is used to find the friction factor that makes the squared difference between the left-hand side and right-hand side zero (Row 11 of **Table 4** and **Table 5**). Rows 1 and 2 are the density and dynamic viscosity of water at 10 degrees Celsius. Using these values of pure water will provide a reasonable estimate for friction factor. Row 10 is pipe roughness for polyvinyl chloride (PVC) pipes. For PVC, a common value is 0.0021 mm (Uni-Bell PVC Pipe Association, 2012). The next row, Row 11, is the relative roughness which is the pipe roughness divided by the pipe diameter.

Table 4. Solving for Friction Factor Using the Colebrook Equation (For Total Flow)

Row #	Properties	English Units	SI Units	Reference (as relevant)
1	Density of Water (10˚C)	62.4 lbm/ft^3	1000 kg/m^3	Elger et al., 2020
2	Dynamic Viscosity of Water (10˚C)	0.00088 lbm/(ft-s)	0.00131 Pa·s	Elger et al., 2020
3	Gravity	32.2 lbm ft/s^2	9.8 m/s^2	Elger et al., 2020
4	Pipe Diameter	0.083 ft	0.025 m	-
5	Cross Sectional Area	0.005 ft^2	0.0005 m^2	-
6	Total Pipe Length	7.83 ft	2.4 m	-
7	Volumetric Flow Rate	0.028 ft^3/s	0.0008 m^3/s	-
8	Average Velocity (Volumetric Flow Rate/Cross Sectional Area)	5.2 ft/s	1.6 m/s	-
9	Reynolds Number (Equation 5)	30,473	-	-
10	Pipe Roughness (PVC Pipe)	0.0000049 ft	0.0021 mm	Uni-Bell, 2012
11	Relative Roughness	5.9E-05	-	-
12	Friction Factor	0.024	-	-
13	LHS of Colebrook Equation	6.52	-	-
14	RHS of Colebrook Equation	6.52	-	-
15	Difference	0	-	-
16	Squared Difference	0	-	-

Table 5. Solving for Friction Factor Using the Colebrook Equation (For 1/4th Total Flow)

Row #	Properties	English Units	SI Units	Reference (as relevant)
1	Density of Water (20 C)	62.4 lbm/ft^3	1000 kg/m^3	Elger et al., 2020
2	Dynamic Viscosity of Water (20 C)	0.00088 lbm/(ft-s)	0.00131 Pa·s	Elger et al., 2020
3	Gravity	32.2 lbm ft/s^2	9.8 m/s^2	Elger et al., 2020
4	Pipe Diameter	0.083 ft	0.025 m	-
5	Cross Sectional Area	0.005 ft^2	0.0005 m^2	-
6	Total Pipe Length	0.5 ft	0.15 m	-
7	Volumetric Flow Rate	0.007 ft^3/s	0.0002 m^3/s	-
8	Average Velocity (Volumetric Flow Rate/Cross Sectional Area)	1.3 ft/s	0.4 m/s	-
9	Reynolds Number (Equation 5)	7,618	-	-
10	Pipe Roughness (PVC Pipe)	0.0000049 ft	0.0021 mm	Uni-Bell, 2012
11	Relative Roughness	5.9E-05	-	-
12	Friction Factor	0.033	-	-
13	LHS of Colebrook Equation	5.48	-	-
14	RHS of Colebrook Equation	5.48	-	-
15	Difference	0	-	-
16	Squared Difference	0	-	-

Once the friction factor is found, then the pipe head loss is predicted with the Darcy-Weisbach equation, **Equation 10**.

$$h_{major} = f \cdot \left(\frac{L}{D}\right) \cdot \left(\frac{v^2}{2 \cdot g}\right) \tag{10}$$

where

L = total pipe length, ft

g = gravitational acceleration, 32.2 ft/s^2

For total flow:

$$h_{major} = 0.024 \cdot \left(\frac{7.83 \text{ ft}}{0.083 \text{ ft}}\right) \cdot \left(\frac{(5.2 \text{ ft/s})^2}{2 \cdot 32.2 \text{ ft/s}^2}\right) = 0.95 \text{ ft}$$

Major Head Loss = 0.95 ft

For 1/4th flow:

$$h_{major} = 0.033 \cdot \left(\frac{0.5 \text{ ft}}{0.083 \text{ ft}}\right) \cdot \left(\frac{\left(1.3 \frac{\text{ft}}{\text{s}}\right)^2}{2 \cdot 32.2 \frac{\text{ft}}{\text{s}^2}}\right) = 0.005 \text{ ft}$$

Major Head Loss = 0.005 ft

Total Major Head Loss = 0.95 ft + 0.005 ft = 0.995 ft = 0.3 m

Minor head loss is predicted with **Equation 11**.

$$h_{minor} = \left(\frac{v^2}{2 \cdot g}\right) \cdot \sum K \tag{11}$$

where

K = loss coefficient for fittings, unitless (Uni-Bell PVC Pipe Association, 2012)

K-values are specific for each of the PVC fittings used in the pipe network of the bench-scale AnBfMBR. It is unitless, and its values can be obtained from standard tables. These

values are also applicable to a specific pipe diameter. The bench-scale AnBfMBR has 6 90-degree elbows (K = 2.06 x 6), 2 standard tees (K = 1.37 x 2), and 1 ball valve (K = 0.05). The minor head loss must once again be split for total flow and 1/4th of the total flow, which means that loss coefficients, K, must be assigned to a specific flow (total or 1/4th).

For total flow:

$$h_{minor} = \frac{(5.2\ ft/s)^2}{2 \cdot 32.2\ ft/s^2} \cdot 8.29$$

$$h_{minor} = 3.48\ ft\ \ (1.06\ m)$$

For 1/4th flow:

$$h_{minor} = \frac{(1.3\ ft/s)^2}{2 \cdot 32.2\ ft/s^2} \cdot 6.86$$

$$h_{minor} = 0.18\ ft\ (0.05\ m)$$

Total Minor Head Loss = 3.48 ft + 0.18 ft = 3.66 ft = 1.12 m

Head loss through an orifice also is a minor head loss predicted with **Equation 12**, which describes approximate discharge through an orifice.

$$Q = 19.636 \cdot C \cdot d_1^2 \cdot \sqrt{h} \cdot \left(\text{for } \frac{d_1}{d_2} < 0.3\right) \qquad (12)$$

where

Q = influent flow, gpm (measured by a flow meter)

d_1 = diameter of orifice opening, in (0.3125 in)

d_2 = diameter of pipe in which orifice is placed, in (1.05 in)

h = differential head at orifice, ft

C = discharge coefficient, unitless, from Cameron Hydraulic Data (Heald, 2018)

$$3.125\ \text{GPM} = 19.636 \cdot 0.96 \cdot 0.3125\ \text{in}^2 \cdot \sqrt{h}$$

$$h = 2.88\ \text{ft}\ (0.88\ \text{m})$$

Table 6. Summary of Head Losses

Static Head Loss	0.88 ft (0.27 m)
Major Head Loss	0.995 ft (0.30 m)
Minor Head Loss	3.66 ft (1.12 m)
Orifice Head Loss	2.88 ft (0.88 m)

Total head loss is the sum of all head losses:

$$\text{Total System Head} = \text{Static Head} + \text{Major Head} + \text{Minor Head} + \text{Orifice Head}$$

$$= 0.88\ \text{ft} + 0.995\ \text{ft} + 3.66\ \text{ft} + 2.88\ \text{ft} = 8.42\ \text{ft} = 2.56\ \text{m}$$

Once head is calculated, it can be input to **Equation 5** to calculate power:

$$P = \gamma \cdot Q \cdot H = (9{,}810\ \text{N/m}^3) \cdot (0.0008\ \text{m}^3\text{/s}) \cdot (2.56\ \text{m}) = 20\ \text{W or } 183\ \text{W/m}^3$$

Then, this can be input into **Equation 6** to calculate the velocity gradient.

$$G = \sqrt{P / \mu \cdot V} = \sqrt{20\ \text{W}/(1.31 \times 10^{-3}\ \text{N} \cdot \text{s/m}^2 \cdot 0.08\ \text{m}^3)} = 373\ 1/\text{s}$$

A key objective of this research effort is the evaluation of different power input values on plastic biofilm carrier membrane scour efficiency and the rate of transmembrane pressure (TMP) buildup. A flow meter was installed to measure the influent flow/rate of recirculation of the bench-scale AnBfMBR. As seen by **Equation 5**, mixing power input

is a function of flow rate. The flow rate could be controlled by a ball valve, as seen in **Figure 16**.

Figure 16. Ball Valve controlling the recirculation flow rate.

2.4.2 Mixing Study

A systematic analysis of mixing for the bench-scale AnBfMBR was conducted with K5 and Z-400 carriers. The purpose was to evaluate the degree of carrier mixing in the bench-scale AnBfMBR at a range of power inputs. It is important to note that experiments with K5 media were conducted at a range of power inputs, but experiments with Z-400 were conducted at a single power input.

For K5 media, the bench-scale AnBfMBR was tested at four different flow rates with clean-water at 15% carrier fill: 5, 8, 10, and 12.5 GPM. Videos were recorded of the bench-scale AnBfMBR in operation and sent to the research team for review. The videos showed very good mixing at 12.5 GPM and good mixing at 10 GPM and 8 GPM. There was no mixing at 5 GPM. It is important to note that the plastic biofilm carriers and

membrane plate interacted at the flow rates of 8, 10, and 12.5 GPM, but not at 5 GPM. Therefore, the power inputs used for testing with K5 media were for 8, 10, and 12.5 GPM.

For Z-400 carriers, a similar systematic analysis was conducted. However, the goal of these tests was to identify a minimum mixing power input, which was established as the single mixing power input for Z-400 carrier experiments. The bench-scale AnBfMBR was tested at six different flow rates with clean-water at 10% carrier fill: 6, 7, 8, 9, 10, and 12.5 GPM. The videos showed that t little mixing and no membrane-biofilm carrier interaction at 6 and 7 GPM. 8 and 9 GPM gave good mixing and membrane-biofilm carrier interaction. 10 and 12.5 GPM gave very good mixing and membrane-biofilm carrier interaction. These tests indicate that 8 or 9 GPM was the minimum value for acceptable mixing. 9 GPM was used for Z-400 carrier experiments because of safety factor to account for good biofilm carrier mixing with biomass in the bench-scale AnBfMBR.

Table 7 presents the power input and velocity gradient for the four flow rates considered in the experiments. Calculations for the flow rate of 12.5 GPM are shown above, and the calculations for the other three flow rates are detailed in **Appendix A**, **B**, and **C**.

Table 7. Summary of Power Input and Velocity Gradient (Entire System)

Flow Rate (GPM)	Power (W and W/m^3)	Velocity Gradient (1/s)
12.5	20 (183)	436
10.0	10 (91)	308
9.0	9 (80)	293
8.0	6 (55)	239

A key assumption is that **Equation 5** should not include energy losses in the pipes and fittings and that power input should be the input to the bench-scale AnBfMBR contents. This assumption includes that orifice loss is a loss to fittings and not power

delivered to the bench-scale AnBfMBR's contents. Therefore, the static head only should be accounted for in **Equation 5**, which provides a minimum value for power and velocity gradient. Calculation of this is shown below for the flow rate of 12.5 GPM. Calculations for the other three flow rates are detailed in **Appendix D**. A summary of the power input and velocity gradient for the four flow rates using this assumption are summarized in **Table 8**.

$$P = \gamma \cdot Q \cdot H = (9{,}810\ N/m^3) \cdot (0.0008\ m^3/s) \cdot (0.27\ m) = 2.1\ W \text{ or } 26\ W/m^3$$

$$G = \sqrt{P / \mu \cdot V} = \sqrt{2.1\ W/(1.31 \times 10^{-3}\ N \cdot s/m^2 \cdot 0.08\ m^3)} = 141\ 1/s$$

Table 8. Summary of Minimum Power Input and Velocity Gradient Assuming that Only the Static Head is Relevant

Flow Rate (GPM)	Power (W, W/m^3)	Velocity Gradient (1/s)
12.5	2.1, 26	141
10.0	1.6, 20	124
9.0	1.5, 19	120
8.0	1.3, 16	111

Table 8 indicates that only accounting for static head in **Equation 5** gives more realistic values, because they align well with generally accepted design criteria for mechanical mixers.

Another possible assumption is that **Equation 5** should include static head and orifice loss. Calculation of this is shown below for the flow rate of 12.5 GPM. Calculations for the other three flow rates are detailed in **Appendix E**. A summary of the power input and velocity gradient for the four flow rates using this assumption are summarized in **Table 9**.

$$P = \gamma \cdot Q \cdot H = (9{,}810\ N/m^3) \cdot (0.0008\ m^3/s) \cdot (0.27+0.88\ m) = 9\ W \text{ or } 113\ W/m^3$$

$$G = \sqrt{P / \mu \cdot V} = \sqrt{9\ W/(1.31 \times 10^{-3}\ N \cdot s/m^2 \cdot 0.08\ m^3)} = 293\ 1/s$$

Table 9. Summary of Minimum Power Input and Velocity Gradient Assuming that both the Static Head and Orifice Loss is Relevant

Flow Rate (GPM)	Power (W, W/m^3)	Velocity Gradient (1/s)
12.5	9, 113	293
10.0	6, 61	239
9.0	4, 50	195
8.0	3, 39	169

The values in **Table 7** correspond to maximum values of power input and velocity gradient. The most accurate estimates of the actual mixing input lie closer to the values in **Table 6**.

It is important to note that the head loss (inefficiency) of a mechanical mixer is minimal. Thus, to compare inputs we also consider the system demands without major and minor head losses so that we may compare to mechanical mixing. The information in this report demonstrates that a hydraulic mixing system that incurs head loss due to anything beyond the pump motor will be less efficient than mechanical mixing.
The two important points that emerge from this mixing evaluation are: 1) confirmed that a 15-20 W/m^3 power input is required to mix plastic biofilm carriers and 2) mechanical mixers are more cost effective than a hydraulic mixing system.

2.5 Experimental Design

Experiments were conducted following a 'run to failure' method, in which the ceramic membranes provide filtration, and the time it takes to reach a 'failure transmembrane pressure (TMP)' is recorded. Membrane TMP is important in this research because it indicates membrane performance in terms of fouling that leads to failure. Membrane permeate flux, TMP, and time were recorded on a data-logging program that was electrically connected to the bench-scale AnBfMBR. The failure TMP

for this research effort was set at 35 kPa (0.35 atm = 5.08 psig) because the value is close to the criterion in previous literature. 30 kPa (0.30 atm = 4.41 psig) is a criterion listed in Rittmann and McCarty (2020), and 30 kPa also was the failure TMP used in Lee, Kang, and Lee (2006) and Jin, Ong, and Ng (2013).

3. Physical Characteristics of Plastic Biofilm Carriers

3.1 Scope and Purpose

In this section is an experimental evaluation of Veolia's K5, Z-200, and Z-400 plastic carriers to determine mass-based specific surface area (SSA) and water displacement (Di) by adding plastic carriers to a bioreactor. Surface area is defined here as that which is exposed to water and nutrients and is able to accumulate biofilm. Water-displacement ratio (Di) is defined here as the water volume displaced by plastic carriers to volume of added carriers. Defining SSA is important because it allows biofilm reactor modelers and designers to associate biofilm area and plastic carrier volume. The total plastic carrier volume that is required can then be applied to evaluate its impact on bioreactor volume. The volume of water displaced by plastic carriers, or Di, in a fixed volume is important because it allows designers to define the extent of reaction volume reduction due to plastic carriers.

K5 carriers have SSA units that are based on their unit volume (i.e., m^2 of biofilm/m^3 of K5 carrier, or m_F^2/m_C^3). Z-carriers have SSA units that are based on the number of plastic carriers (i.e., m^2 of biofilm/million pieces (mp) of Z-carriers, or m_F^2/mp). Z-carrier's SSA is based on the number of plastic carriers because their hyperboloid shape results in, depending on their orientation when packed, the same mass of Z-carriers occupying different volumes. The volume of one-million Z-carrier pieces ranges from 1.3 to 2.0 m^3 per million pieces (mp) (Veolia, France). Thus, we seek to define Z-carrier SSA normalized to its mass. Additionally, we seek to define how Z-carrier SSA fluctuates with plastic carrier volume. It is important to note the units in the table, specifically m_C^3, m_F^3, m_R^3, and m_W^3, which will be used throughout this section. 'C' represents biofilm carrier,

'F' represents biofilm carrier fill, 'R' represents bioreactor, and 'W' represents water or liquid.

3.1.1. Carrier Specific Surface Area (SSA)

Experiments to determine carrier mass and volume are crucial for determining mass-based plastic carrier SSA. Detailed information on the results of the mass and volume experiments are presented in the following two sections.

Equation 13 defines mass-based SSAs ($SSA_{M,c}$) for K5, Z-200, and Z-400 carriers in terms of m^2 surface area per kg of the carrier. $SSA_{M,c}$ can be calculated by dividing a volume-based SSA (SSA_V) by a plastic carrier density (ρ_c). This can be expressed as:

$$SSA_{M,c}=SSA_{V,c}/\rho_c \tag{13}$$

where

$SSA_{M,c}$=mass-based SSA of carrier type c, m_F^2/kg_C

$SSA_{V,c}$=volume-based SSA of carrier type c, m_F^2/m_C^3

ρ_c=density of carrier type c, kg_C/m_C^3

3.1.2. Carrier Mass

The considered carriers (i.e., K5, Z-200, and Z-400) were counted into 50-, 250-, 500, and 1,000-piece samples. The mass of each carrier count sample was measured. The relationships between number of K5, Z-200, and Z-400 pieces and their masses is graphically represented as **Figures F1, F2,** and **F3**. A linear regression analysis concluded that one piece of K5 has a mass 0.36 g (R^2 = 1.000), Z-200 has 0.37 g (R^2 = 0.9998), and Z-400 has 0.38 g (R^2 =1.000). **Tables F1** through **F3** present results of three plastic carrier mass measurements: K5, Z-200, and Z-400. These data are important because they allow

biofilm-reactor designers to determine the number of carriers in a mass of carriers. From that, an SSA can be assigned to any mass of carriers. **Equations 14** through **16** relates number of carriers, total carrier mass, and mass of individual carriers for K5, Z-200, and Z-400 carrier types, respectively.

$$\text{Number of K5 Carriers} = \frac{\text{Mass of K5 (g)}}{0.36 \ \frac{\text{g}}{\text{K5 carrier}}} \tag{14}$$

$$\text{Number of Z-200 Carriers} = \frac{\text{Mass of Z-200 (g)}}{0.37 \ \frac{\text{g}}{\text{Z-200 carrier}}} \tag{15}$$

$$\text{Number of Z-400 Carriers} = \frac{\text{Mass of Z-400 (g)}}{0.38 \ \frac{\text{g}}{\text{Z-400 carrier}}} \tag{16}$$

Linear regression analysis of mass measurements for different carrier count samples were validated by weighing 25 individual pieces. **Table 10** lists the average, minimum, maximum, and standard deviation of measurements for three types of plastic carriers.

Table 10. Individual Plastic Carrier Mass (g/piece), based on measurements of 25 Pieces

	K5	**Z-200**	**Z-400**
Average mass (g)	0.35	0.37	0.37
Minimum mass (g)	0.31	0.35	0.35
Maximum mass (g)	0.40	0.39	0.40
Standard deviation	0.02	0.01	0.01

Table 10 compares the experimental mass, which is the mass determined using a linear regression analysis of the carrier count samples (i.e., 50-, 250-, 500-, and 1,000-piece samples), to the actual mass values, which is the mass of individual pieces.

Table 11. Comparison of Experimental Mass and Actual Mass

	Experimental Mass (g)	**Actual Mass (g)**
K5	0.36 (R^2 = 1.000)	0.35 ± 0.02
Z-200	0.37 (R^2 = 0.9998)	0.37 ± 0.01
Z-400	0.38 (R^2 = 1.000)	0.37 ± 0.01

Table 11 highlights that the experimental mass is very close to the values of actual mass. Therefore, the experimental mass values will be applied throughout this study.

3.1.3. Carrier Volume

The volume occupied by a defined number of carriers was measured using a container of known volume and a defined mass of carriers. This set of experiments was conducted to relate carrier volume and number of carriers.

Method of determining plastic carrier volume:

1. Identify three containers with differing volumes. In this study, three containers with volumes of 710, 946, and 1890 mL were used.
2. Measure and record the mass of each container.
3. Fill each of the three containers with K5 media until filled. Shake the container and fill the container with K5 media until the container is completely filled.

4. Measure and record the mass of each container (with K5 media).
5. Use **Equations 14, 15, and 16,** to calculate the number of carriers that are associated with a recorded mass. These equations can be used to calculate the number of carriers for any mass of carriers.
6. Repeat for Z-200 and Z-400 carriers.

For each carrier type, relationships between number of pieces, their volume, and their mass are graphically presented as **Figures G1, G2, G3, G4, G5,** and **G6**. A linear-regression analysis was conducted to determine the volume of any number or mass of plastic carriers. Carrier mass data reported in the previous section has been used to develop **Equations 17** through **22**. The coefficients in these equations were determined by linear regression analysis. **Tables G1, G2,** and **G3** present results of the plastic carrier volume measurements.

Carrier volume from a known number of carriers

$$\text{Volume of K5 Carriers } (m^3) = \frac{\text{Number of K5 pieces}}{314{,}000 \ \frac{\#}{m^3}} \tag{17}$$

$$\text{Volume of Z-200 Carriers } (m^3) = \frac{\text{Number of Z-200 pieces}}{604{,}000 \ \frac{\#}{m^3}} \tag{18}$$

$$\text{Volume of Z-400 Carriers } (m^3) = \frac{\text{Number of Z-400 pieces}}{614{,}000 \ \frac{\#}{m^3}} \tag{19}$$

Carrier volume from a known mass of carriers

$$\text{Volume of K5 Carriers } (m^3) = \frac{\text{Mass of K5 (g)}}{114{,}000\ \frac{g}{m^3}} \quad (20)$$

$$\text{Volume of Z-200 Carriers } (m^3) = \frac{\text{Mass of Z-200 (g)}}{223{,}000\ \frac{g}{m^3}} \quad (21)$$

$$\text{Volume of Z-400 Carriers } (m^3) = \frac{\text{Mass of Z-400 (g)}}{232{,}000\ \frac{g}{m^3}} \quad (22)$$

3.1.4. Results and Discussion of Carrier Mass and Volume Experiments

The mass relationships and the data acquired from conducting the volume experiments were used to calculate mass-based plastic carrier SSA. Thereby, relationships between carrier number, mass, and volume were obtained. Three calculations examples are shown below to compute the mass-based plastic carrier SSA for K5, Z-200, and Z-400 carriers. Additionally, calculations are shown to find the number of plastic carriers per kilogram.

Example: Finding the mass-based plastic carrier SSA of K5 carriers (Use Equation 13)

$$SSA_{M,c} = SSA_{V,c}/\rho_c$$

Equation 20 can be used to determine the volume associated with a known mass of K5 carriers:

$$\text{Volume of K5 Carriers } (m^3) = \frac{\text{Mass of K5 (g)}}{114{,}000\ \frac{g}{m^3}} = \frac{86\ g}{114{,}000\ \frac{g}{m^3}}$$

$$= 7.54 \times 10^{-4}\ m^3$$

$$SSA_{M,K5}=800\frac{m_F^2}{m_C^3}\cdot\frac{7.54\text{ x }10^{-4}\text{ m}^3\text{ of K5 carriers}}{0.086\text{ kg of K5 carriers}}=\mathbf{7.0}\,\frac{\mathbf{m_F^2}}{\mathbf{kg}}$$

Example: Finding the mass-based plastic carrier of Z-200 carriers (Use Equation 13)

$$SSA_{M,c}=SSA_{V,c}/\rho_c$$

Equation 18 can be used to determine the volume associated with 1 mp of Z-200 carriers:

$$\text{Volume of Z-200 Carriers (m}^3)=\frac{\text{Number of Z-200 pieces}}{604{,}000\ \frac{\#}{m^3}}=\frac{\text{1 mp of Z-200 carriers}}{604{,}000\ \frac{\#}{m^3}}=1.66\text{ m}^3$$

Equation 21 can then be used to determine the mass associated with a known volume of Z-200 carriers:

$$\text{Volume of Z}-200\text{ Carriers (m}^3)=\frac{\text{Mass of Z}-200\text{ (g)}}{223{,}000\ \frac{g}{m^3}}$$

$$=1.66\text{ m}^3\cdot 223{,}000\ \frac{g}{m^3}=370{,}000\text{ g}=370\text{ kg}$$

$$SSA_{M,Z-200}=1{,}500\frac{\text{m}^2\text{ of biofilm growth area}}{\text{mp of Z}-200\text{ carriers}}\cdot\frac{\text{1 mp of Z}-200\text{ carriers}}{1.66\text{ m}^3}$$

$$\cdot\frac{1.66\text{ m}^3}{370\text{ kg}}=\mathbf{4.1\ m_F^2/kg}$$

Example: Finding the mass-based plastic carrier of Z-400 carriers (Use Equation 13)

$$SSA_{M,c}=SSA_{V,c}/\rho_c$$

Equation 19 can be used to determine the volume associated with 1 mp of Z-400 carriers:

$$\text{Volume of Z} - 400 \text{ Carriers } (\text{m}^3) = \frac{\text{Number of Z}-400 \text{ pieces}}{614{,}000 \frac{\#}{\text{m}^3}} =$$

$$\frac{1 \text{ mp of Z-400 carriers}}{614{,}000 \frac{\#}{\text{m}^3}} = 1.63 \text{ m}^3/\text{mp}$$

Equation 22 can then be used to determine the mass associated with a known volume of Z-400 carriers:

$$\text{Volume of Z} - 400 \text{ Carriers } (\text{m}^3) = \frac{\text{Mass of Z} - 400 \text{ (g)}}{232{,}000 \frac{\text{g}}{\text{m}^3}}$$

$$= 1.63 \text{ m}^3 \cdot 232{,}000 \frac{\text{g}}{\text{m}^3} = 378{,}000 \text{ g} = 378 \text{ kg}$$

$$\text{SSA}_{\text{M,Z}-400} = 1{,}500 \frac{\text{m}^2 \text{ of biofilm growth area}}{\text{mp of Z} - 400 \text{ carriers}} \cdot \frac{1 \text{ mp of Z} - 400 \text{ carriers}}{1.63 \text{ m}^3}$$

$$\cdot \frac{1.63 \text{ m}^3}{378 \text{ kg}} = \mathbf{4.0\ m_F^2/kg}$$

Finding the number of K5, Z-200, and Z-400 pieces per kilogram (Use Equations 24 – Equation 16)

$$\text{Number of K5 Carriers} = \frac{\text{Mass of K5 (g)}}{0.36 \frac{\text{g}}{\text{K5 carrier}}} = \frac{1000 \text{ g}}{0.36 \frac{\text{g}}{\text{K5 carrier}}}$$

$$= \mathbf{2{,}800\ pieces/kg}$$

$$\text{Number of Z} - 200 \text{ Carriers} = \frac{\text{Mass of Z} - 200 \text{ (g)}}{0.37 \frac{\text{g}}{\text{Z} - 200 \text{ carrier}}}$$

$$= \frac{1000 \text{ g}}{0.37 \frac{\text{g}}{\text{Z} - 200 \text{ carrier}}} = \mathbf{2{,}700\ pieces/kg}$$

$$\text{Number of Z} - 400 \text{ Carriers} = \frac{\text{Mass of Z} - 400 \text{ (g)}}{0.38 \frac{\text{g}}{\text{Z} - 400 \text{ carrier}}}$$

$$= \frac{1000 \text{ g}}{0.38 \frac{\text{g}}{\text{Z} - 400 \text{ carrier}}} = \mathbf{2,600 \text{ pieces/kg}}$$

3.2. Carrier Displacement

The addition of plastic carriers to a fixed volume displaces liquid volume. The extent of water displacement depends on the plastic carrier's characteristics. K5, for example, has an open structure. Thus, the volume occupied by these plastic carriers is much greater than the water volume displaced by the plastic used to fabricate plastic carriers. Here, we seek to determine the volume of water displaced by K5, Z-200, and Z-400 carriers. Steps for determining plastic-carrier displacement are listed below.

3.2.1. Materials and Methods

Materials:

- K5, Z-200, and Z-400 carriers (each using 50-, 250-, 500-, and 1,000-piece samples)
- 11-L graduated container
- Digital laboratory scale
- Ruler

Method of determining plastic carrier displacement:

1. Fill an empty 11-L graduated container, which is pictured in **Figure 17,** with 8 L of water. It is important to note that the images in **Figure 17** show that the sides of the container are sloped. This did not have an impact in displacement and water volume calculations.

2. The starting water elevation, which is in the "8-L" label, is shown in **Figure 17**. This will be the same for all displacement experiments.
3. Insert a defined number of plastic carriers into the water-filled container.
4. Record the difference in water surface elevation with a ruler.
5. Agitate the carrier and water filled container and re-record the difference in water surface elevation. Repeat three times (EL1, EL2, EL3).
6. Calculate the volume of water displaced.

$$\text{volume of liquid displaced} = \text{difference in water surface elevation} \cdot \text{container area}$$

7. Calculate ratio of water volume displaced to original water volume.
8. Repeat steps 1 through 7 for K5, Z-200, and Z-400 carriers.

Figure 17. 11-L graduated container with 8-L of water.

3.2.2. Results of Displacement Experiments

Figures H1 through **H3** and **Tables H1** through **H3** present displacement experiments results. The results indicate a linear relationship between the number of carriers and volume of liquid they displaced. **Equations 23** through **25** establish relationships between the volume of liquid displaced and number of carriers.

$$\text{Volume of Liquid Displaced: K5 Carriers } \left(m_W^3\right) = 6 \times 10^{-7} \ \frac{m_W^3}{\#} \cdot \text{Number of K5 Carriers} \quad (23)$$

$$\text{Volume of Liquid Displaced: Z-200 Carriers } \left(m_W^3\right) = 4 \times 10^{-7} \ \frac{m_W^3}{\#} \cdot \text{Number of Z-200 Carriers} \quad (24)$$

$$\text{Volume of Liquid Displaced: Z-400 Carriers } \left(m_W^3\right) = 4 \times 10^{-7} \ \frac{m_W^3}{\#} \cdot \text{Number of Z-400 Carriers} \quad (25)$$

Displacement in a range of 0% and 100% carrier fill can be determined for K5, Z-200, and Z-400 carriers. Carrier fill (F) is the plastic carrier volume in a bioreactor liquid volume, or m^3 of biofilm carrier per m^3 of bioreactor (m_C^3/m_R^3). This is an important parameter, because it allows one to determine the volume of plastic carriers in a bioreactor. **Table I1, I2, and I3** in Appendix I presents the mass-based plastic carrier displacement values for a range of 0% to 100% carrier fill of K5, Z-200, and Z-400 carriers. One can see that the displacement at 100% fill is 0.188 which is comparable with the displacement value of 0.18 reported by Veolia. **Table 12** highlights the displacement at 100% fill for K5, Z-200, and Z-400 carriers.

Table 12. Displacement of Biofilm Carriers at 100% Fill

Car - rier	Percent Fill (%)	Total Water Volume (m3)	Actual Water Volume (m3)	Number of Pieces	Mass of Pieces (g)	Volume of Liquid Displaced (m3)	Di (m_W^3/m_C^3)
K5	100	0.08	0.08	25120	9120	0.015072	0.188
Z-200	100	0.08	0.08	48320	17840	0.019328	0.242
Z-400	100	0.08	0.08	49120	18560	0.019648	0.246

Example: Finding Di of K5 Carriers at 100% Fill (Use Equation 17 and 23)

$$\text{Volume of Liquid Displaced: K5 Carriers } \left(m^3_W\right) = 6 \times 10^{-7} \frac{m^3_W}{\#} \cdot \text{Number of K5 Carriers}$$

Equation 17 can be used to determine the number of carriers associated with 1 m^3 of K5 carriers:

$$\text{Volume of K5 Carriers } (m^3) = \frac{\text{Number of K5 pieces}}{314{,}000 \frac{\#}{m^3}} = 1\ m^3 * 314{,}000 \frac{\#}{m^3} = 314{,}000 \text{ pieces}$$

Then, plug into **Equation 23**:

$$\text{Volume of Liquid Displaced: K5 Carriers } \left(m^3_W\right) = 6 \times 10^{-7} \frac{m^3_W}{\#} \cdot \text{Number of K5 Carriers}$$

$$= 6 \times 10^{-7} \frac{m^3_W}{\#} * 314{,}000 \text{ pieces} = \mathbf{0.188\ m^3_W / m^3_C}$$

Example: Finding Di of Z-200 Carriers at 100% Fill (Use Equation 18 and 24)

$$\text{Volume of Liquid Displaced: Z-200 Carriers } \left(m^3_W\right) = 4 \times 10^{-7} \frac{m^3_W}{\#} \cdot \text{Number of Z-200 Carriers}$$

Equation 18 can be used to determine the number of carriers associated with 1 m^3 of Z-200 carriers:

$$\text{Volume of Z-200 Carriers } (m^3) = \frac{\text{Number of Z-200 pieces}}{604{,}000 \frac{\#}{m^3}} = 1\ m^3 * 604{,}000 \frac{\#}{m^3} = 604{,}000 \text{ pieces}$$

Then, plug into **Equation 24:**

$$\text{Volume of Liquid Displaced: Z-200 Carriers } \left(m^3_W\right) = 4 \times 10^{-7} \frac{m^3_W}{\#} \cdot \text{Number of Z-200 Carriers}$$

$$= 4 \times 10^{-7} \frac{m^3}{\#} * 604{,}000 \text{ pieces} = \mathbf{0.242\ m^3_W / m^3_C}$$

Example: Finding Di of Z-400 Carriers at 100% Fill (Use Equation 19 and 25)

$$\text{Volume of Liquid Displaced: Z-400 Carriers } \left(m^3_W\right) = 4 \times 10^{-7} \frac{m^3_W}{\#} \cdot \text{Number of Z-400 Carriers}$$

Equation 19 can be used to determine the number of carriers associated with 1 m^3 of Z-400 carriers:

$$\text{Volume of Z-400 Carriers } (m^3) = \frac{\text{Number of Z-400 pieces}}{614{,}000\ \frac{\#}{m^3}}$$

$$= 1\ m^3 * 614{,}000 \frac{\#}{m^3} = 614{,}000 \text{ pieces}$$

Then, plug into **Equation 25:**

$$\text{Volume of Liquid Displaced: Z-400 Carriers } \left(m^3_W\right) = 4 \times 10^{-7}\ \frac{m^3_W}{\#} \cdot \text{Number of Z-400 Carriers}$$

$$4 \times 10^{-7} \frac{m^3}{\#} * 614{,}000 \text{ pieces} = \mathbf{0.246\ m^3_W / m^3_C}$$

4. Effects of Mixed Liquor Suspended Solids (MLSS) and Carriers on Permeate Flux

4.1. Methods for K5 Media Experiments and Z-400 Carrier Experiments

I carried out series of permeate-flux experiments with K5 and Z-400 carriers. **Table 13** lists the ranges of variables tested for K5, and **Table 14** lists the ranges of variables tested for Z-400. The K5 media experiments had a total of 45 tests. The Z-400 carrier experiments had a total of 40 tests. Methods for the two sets of experiments, described below, were similar for the two carriers.

Table 13. Ranges of Main Variables for K5 Experiments

MLSS Concentration (mg/L)	1,000, 3,000, 5,000, 7,500, and 10,000
Carrier Fill (%)	0, 20, and 40
Power Input (W/m^3)	16, 20, and 26
Permeate Flux	1.0 $m^3/d.m^2$

Table 14. Ranges of Main Variables for Z-400 Experiments

MLSS Concentration (mg/L)	1,000, 3,000, 5,000, 7,500, and 10,000
Carrier Fill (%)	0, 20, 40, and 60
Power Input (W/m^3)	19
Permeate Flux	0.25 and 1.0 $m^3/d.m^2$

Method for the K5 Experiments:

1. Insert the appropriate amount of clean water and AD sludge into the bench-scale AnBfMBR, following **Equation 1** and **Equation 2**
2. Measure and record the temperature of the diluted sludge inside the bench-scale AnBfMBR
3. Turn on the recirculation pump
4. Twist the ball valve on the recirculation system until the desired flow rate is achieved

5. Start-up the datalogging program and begin recording data (i.e., transmembrane pressure and permeate flow rate)
6. Set the permeate pump speed to Speed 4, turn on the permeate pump, and monitor datalogging program until the TMP reaches 35 kPa (0.35 atm = 5.08 psig), then turn off the permeate pump
7. Backwash the ceramic membrane module for a minimum of 15 seconds
8. Twist the ball valve on the recirculation system until the flow rate of 10 GPM and 8 GPM is achieved and repeat Steps 3-7
9. Insert K5 carriers into the bench-scale AnBfBMR to achieve a 20% carrier fill, then repeat steps 3-8
10. Insert K5 carriers into the bench-scale AnBfMBR to achieve a 40% carrier fill, then repeat steps 3-8
11. Clean the bench-scale AnBfMBR, ceramic membranes, and K5 media

Method for Z-400 Carriers Experiments:

1. Insert the appropriate amount of clean water and AD sludge into the bench-scale AnBfMBR, following **Equation 1** and **Equation 2**
2. Measure and record the temperature of the diluted sludge inside the bench-scale AnBfMBR
3. Turn on the recirculation pump
4. Twist the ball valve on the recirculation system until the desired flow rate is achieved

5. Start-up the datalogging program and begin recording data (i.e., transmembrane pressure and permeate flow rate)
6. Set the permeate pump speed to Speed 2, turn on the permeate pump, and monitor datalogging program until the TMP reaches 35 kPa (0.35 atm = 5.08 psig), then turn off the permeate pump
7. Backwash the ceramic membrane module for a minimum of 15 seconds
8. Repeat steps 3-7 using a permeate pump speed of Speed 4
9. Insert Z-400 carriers into the bench-scale AnBfBMR to achieve a 20% carrier fill, then repeat steps 3-8
10. Insert Z-400 carriers into the bench-scale AnBfBMR to achieve a 40% carrier fill, then repeat steps 3-8
11. Insert Z-400 carriers into the bench-scale AnBfBMR to achieve a 60% carrier fill, then repeat steps 3-8
12. Clean the bench-scale AnBfMBR, ceramic membranes, and K5 media

4.2. K5 Media Experimental Results and Discussion

Tables 15 through **19** present K5-media experimental results. A total of 45 tests were conducted, and each table presents the time to the failure TMP (35 kPa = 0.35 atm = 5.08 psig) of the ceramic membranes; the permeate flux was 1.0 m/d in all cases. The MLSS concentration tested, which ranges from 1,000 mg/L to 10,000 mg/L, is the only differentiating factor in the tables.

Table 15. Time to Failure TMP (MLSS = 1,000 mg/L)

Power input	0% Carrier Fill	20% Carrier Fill	40% Carrier Fill
16 W/m^3	33 seconds	111 seconds	232 seconds
20 W/m^3	327 seconds	103 seconds	488 seconds
26 W/m^3	433 seconds	552 seconds	583 seconds

Table 16. Time to Failure TMP (MLSS = 3,000 mg/L)

Power input	0% Carrier Fill	20% Carrier Fill	40% Carrier Fill
16 W/m^3	203 seconds	314 seconds	294 seconds
20 W/m^3	263 seconds	731 seconds	309 seconds
26 W/m^3	210 seconds	309 seconds	786 seconds

Table 17. Time to Failure TMP (MLSS = 5,000 mg/L)

Power Input	0% Carrier Fill	20% Carrier Fill	40% Carrier Fill
16 W/m^3	51 seconds	106 seconds	172 seconds
20 W/m^3	49 seconds	114 seconds	156 seconds
26 W/m^3	93 seconds	292 seconds	340 seconds

Table 18. Time to Failure TMP (MLSS = 7,500 mg/L)

Power input	0% Carrier Fill	20% Carrier Fill	40% Carrier Fill
16 W/m^3	69 seconds	131 seconds	134 seconds
20 W/m^3	90 seconds	130 seconds	289 seconds
26 W/m^3	223 seconds	140 seconds	262 seconds

Table 19. Time to Failure TMP (MLSS = 10,000 mg/L)

Power Input	0% Carrier Fill	20% Carrier Fill	40% Carrier Fill
16 W/m^3	15 seconds	38 seconds	187 seconds
20 W/m^3	18 seconds	232 seconds	313 seconds
26 W/m^3	11 seconds	121 seconds	186 seconds

The two key and expected trends are that the time to failure TMP decreased as the MLSS concentration increased, but more carrier fill increased the time to failure TMP. For example, **Table 15** shows that, for the entire range of carrier fill at a power input of 16 W/m^3, greater carrier fill always led to an increase in operation period. This same trend is seen at a power input of 26 W/m^3. Even though the power input of 20 W/m^3 had two exceptions from the five MLSS concentrations, the important trend for all the experiments is that the impact of adding carriers was relatively greater for higher MLSS concentration.

The impact of different power inputs also is interesting. Logically, the time to failure TMP is expected to decrease as the power input is increased because the increased power mixes the carriers faster than a lower power input. However, this trend was not consistently observed in the experiments results. Nonetheless, a power input of 26 W/m^3 always was effective for extending time to TMP failure without carriers, especially at lower MLSS concentrations, e.g., **Table 15**. As the MLSS concentration went to 10,500 mg/L, higher power input failed to increase time to TMP failure with or without carriers. This trend links to a "sweet spot" condition, which is discussed in a following section.

4.3. Z-400 Carrier Experimental Results and Discussion

Tables 20 through **24** present the experimental results for the Z-400 carriers. A total of 40 tests were conducted, and each table presents the time to failure TMP (35 kPa = 0.35 atm = 5.08 psig) of the ceramic membranes. The MLSS concentration tested, which ranges from 1,000 mg/L to 10,000 mg/L, is the only differentiating factors in **Tables 20** through **24.** However, the Z-400 carrier were evaluated for two permeate fluxes: 0.25-m/d and 1.0-m/d. The permeate flux of 0.25-m/d is considered the sustainable flux to

operate at for AnMBRs (Smith et al., 2014), while 1-m/d is considered an upper limit. An additional carrier fill percentage of 60% was tested, but only one power input was tested, 19 W/m^3.

Table 20. Time to Failure TMP (MLSS = 1,000 mg/L)

Permeate Flux	0% Carrier Fill	20% Carrier Fill	40% Carrier Fill	60% Carrier Fill
0.25 m/d	23 min	32 min	2 h 46 min	2 h 43 min
1 m/d	10 min	5 min	12 min	9 min

Table 21. Time to Failure TMP (MLSS =3,000 mg/L)

Permeate Flux	0% Carrier Fill	20% Carrier Fill	40% Carrier Fill	60% Carrier Fill
0.25 m/d	31 min	52 min	2 h 8 min	2 h 21 min
1 m/d	7 min	16 min	24 min	34 min

Table 22. Time to Failure TMP (MLSS = 5,000 mg/L)

Permeate Flux	0% Carrier Fill	20% Carrier Fill	40% Carrier Fill	60% Carrier Fill
0.25 m/d	22 min	28 min	1 h 36 min	1 h 48 min
1 m/d	6 min	15 min	19 min	22 min

Table 23. Time to Failure TMP (MLSS = 7,500 mg/L)

Permeate Flux	0% Carrier Fill	20% Carrier Fill	40% Carrier Fill	60% Carrier Fill
0.25 m/d	26 min	29 min	1 h 31 min	1 h 35 min
1 m/d	9 min	11 min	14 min	15 min

Table 24. Time to Failure TMP (MLSS = 10,000 mg/L)

Permeate Flux	0% Carrier Fill	20% Carrier Fill	40% Carrier Fill	60% Carrier Fill
0.25 m/d	20 min	22 min	51 min	52 min
1 m/d	9 min	11 min	10 min	9 min

The results in **Tables 20** through **24** align with the expected trends: Increased carrier fill significantly extended the operating period, while a higher MLSS decreased the time to failure TMP. Another main takeaway from these results is that a membrane permeate flux of 1.0-m/d led to a substantially shorter time to failure TMP than did 0.25-m/d: a more than 5-fold decrease in the time to failure TMP.

Figure 18 visualizes the effects of MLSS and carrier fill for the Z-400 carriers. The figure presents experimental results that compare the ratio of operating time to reach a failure TMP with and without plastic biofilm carriers, as well as for different MLSS concentrations and plastic-biofilm carrier volumetric fills. The obvious impacts of increasing MLSS making the time to failure shorter and the compensating effect of more carrier fill are readily observable in the top panel for a permeate flux of 0.25 m/d. The strong impact of the higher permeate flux can be seen by comparing the top and bottom panels. It is also important to note some "odd" results. The bottom panel of **Figure 18** has two points that do not follow the expected trend of longer operating time with increasing carrier fill: a MLSS concentration of 1,000 mg/L at a carrier fill of 20% and 60%. Experiments with an MLSS concentration of 1,000 mg/L were conducted first, which may have resulted in some start-up-related deficiencies, such as the ceramic membranes not having been backwashed or cleaned adequately.

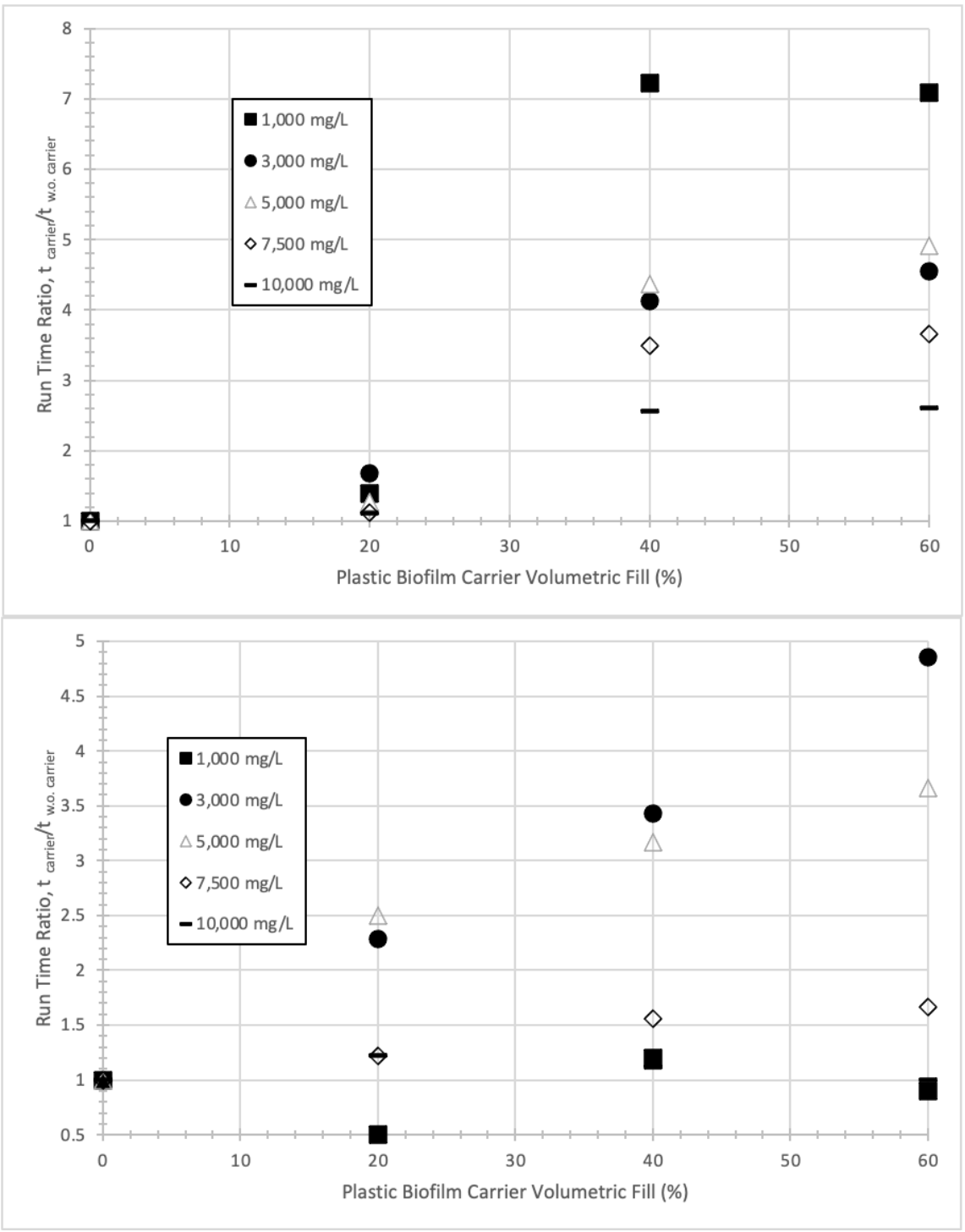

Figure 18. Experimental results that compare the ratio of run time to failure TMP (0.35 atm) with different plastic biofilm carrier volumetric fills and different suspended solids concentrations. Top panel – 0.25 m/d permeate flux; Bottom panel – 1.0 m/d permeate flux

Figure 19 is similar to Figure 18, but compares K5 media to Z-400 carriers at the same permeate flux of 1.0-m/d. The impact of increasing MLSS making the time to failure shorter and the compensating effect of more carrier fill are most clearly observable in the bottom panel for Z-400 carriers than in the top panel for the K5 media. In the top panel, this trend is clearly seen at an MLSS concentration of 10,000 mg/L, which is the highest concentration tested. At lower concentrations, the trend is not as strong.

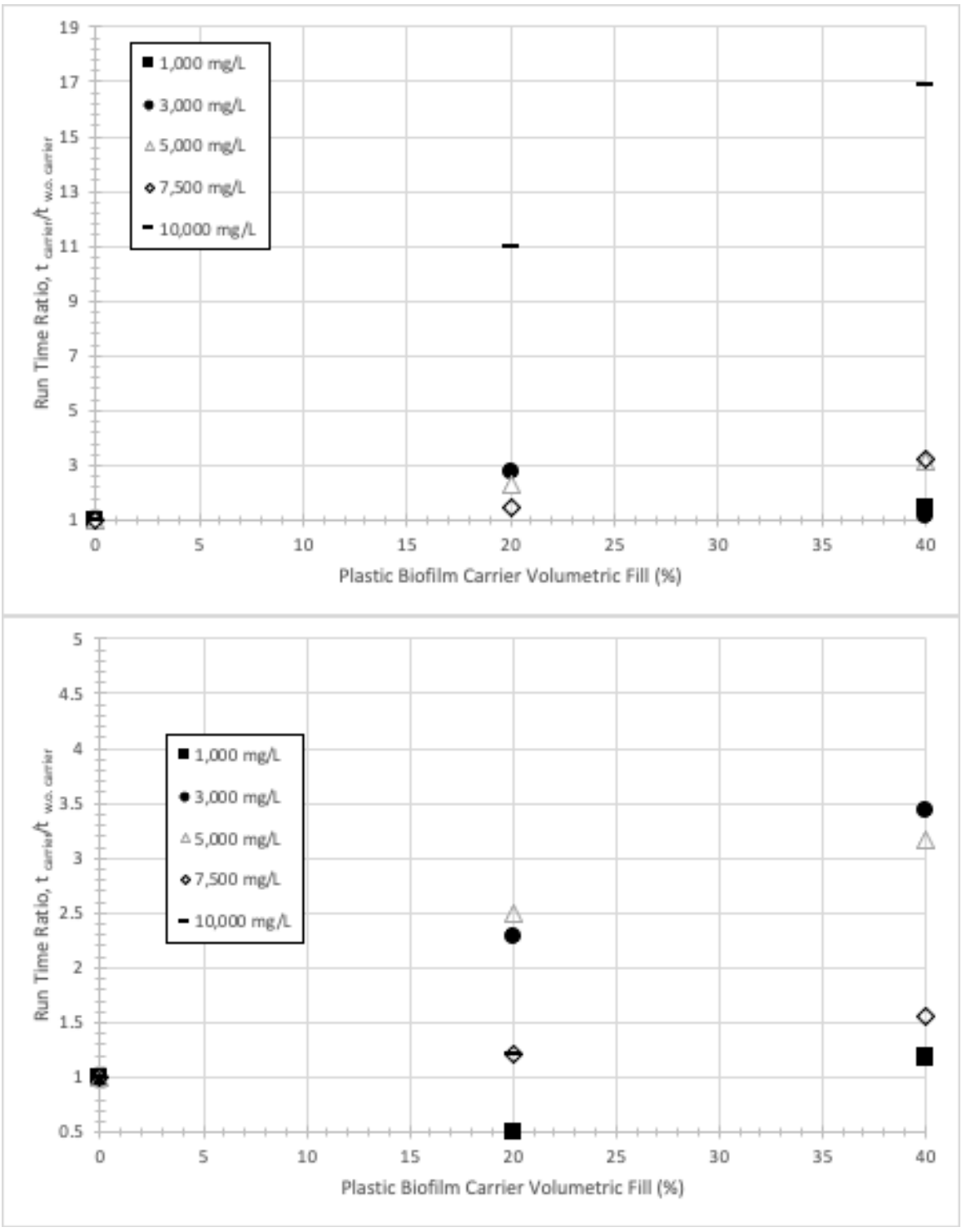

Figure 19. Experimental results that compare the ratio of run time to failure TMP (0.35 atm) with different plastic biofilm carrier volumetric fills and different suspended solids concentrations at a permeate flux of 1.0-m/d. Top panel – K5 Media; Bottom panel – Z-400 Carrier

4.4. "Sweet Spot" Evaluation

A useful interpretation of all the results is finding a "sweet spot," or optimal operating conditions. For the Z-400 carriers, **Tables 22** and **23** demonstrate that the time to failure TMP remained greater than 1.5 h with MLSS concentration between 5,000 mg/L and 7,500 mg/L, a 40% Z-carrier fill, and a membrane permeate flux of 0.25-m/d. 60% carrier fill increased the failure time by only a small amount, but 20% fill led to a sharp decline in failure time. This highlights the "sweet spot" at 40% fill, which is is well below the reported maximum fill: According to McQuarrie and Boltz (2011), the maximum carrier fill in a moving bed bioreactor (MBBR) is 67%. **Figure 18** showcases an approximately 4:1 improvement when compared to a control (i.e., no carrier fill, as in an AnMBR) with the "sweet spot" conditions (e.g., MLSS concentration between 5,000 mg/L and 7,500 mg/L, a 40% Z-carrier fill, and a membrane permeate flux of 0.25-m/d).

For the K-5 carrier, the "sweet spot" was an MLSS concentration between 7,500 mg/L and 10,000 mg/L, a 40% carrier fill, and a power input of 20 W/m^3 when the membrane permeate flux was 1.0 m/d. It is important to note than only a single permeate flux value was tested for the K5 experiments. However, it is expected that the operating time would have increased if a permeate flux of 0.25 m/d were tested. Additionally, the maximum carrier fill tested was 40% for K-5, unlike the Z-400 experiments that had tests with a maximum carrier fill of 60%. The "sweet spot" for the K5 carrier has an average time to failure TMP of about 250 seconds.

These "sweet spot" interpretations have important implications for performance and cost. First, a greater MLSS concentration equates to a smaller bioreactor, which means a smaller footprint and lower capital cost. Second, a lower carrier fill equates to less

capital cost for carriers. These first two factor complement each other, because a smaller volume requires fewer carriers no matter the fill percentage. Lastly, the time to failure TMP using a permeate flux of 0.25-m/d was significantly longer than for 1.0-m/d. With the lower permeate flux, the "sweet spot" has a 1.5- to 2.0-hour operating period before the failure TMP. In practice, the membranes would then need to be *in situ* cleaned by gas sparging. Assuming that the sparging periods last 15 minutes and occur after 1 h 45 min., the total duration of sparging would be only 3 h per day, which is a low amount of time that saves on the energy cost of compressing and sparging the gas. Sustaining a permeate flux of 0.25-m/d in the experiments and having it be the "sweet spot" flux value is noteworthy, because the AnBfMBR technology can have performance standards that align with the AeMBR: 0.25-m/d as reported by Smith et al. (2014).

Overall, an operating flux of 0.25-m/d, a failure TMP of 0.3-atm pressure, MLSS of 5,000 – 7,500 mg/L, and make 40% carrier fill make the AnBfMBR technology technically and economically viable using the Z-400 carriers.

5. Summary and Recommendations

5.1. Summary

High-strength wastes (e.g., food-processing wastewater) pollute waters and emit green-house gases. They increase production costs, and their discharges are commonly regulated. A number of state-of-the-art anaerobic bioreactors have promise for intensified anaerobic biological treatment and energy recovery, but they have drawbacks. The AnBfMBR presents an improvement to a state-of-the-art AnMBR technology. The AnBfMBR is a hybrid suspended-growth and biofilm reactor: its two main components are plastic biofilm carriers and membranes. Ceramic-plate UF membranes are integrated with suspended biomass and plastic-biofilm carriers for liquid and solids separations. Plastic-biofilm carriers continuously scour membranes surfaces, thereby, allowing a significantly greater permeate flux than a state-of-the-art AnMBR. The plastic biofilm carriers provide the surface onto which the biofilms grow. Membranes provide liquid-solid separation, retention of suspended biomass, and a solids-free effluent. Introducing sufficient surface area promotes the biofilm accumulation of slow-growing methanogens that convert volatile fatty acids into methane gas. Biofilms growing on these surfaces will have a mixed culture that primarily consists of methanogens and inert particulate solids, but also includes some acetogens. Biomass that detaches from biofilms become a component of the suspended growth.

The primary objective of this thesis project was to evaluate the ability of plastic biofilm carriers to minimize ceramic-membrane fouling in the AnBfMBR setting. In Chapter 3, I evaluated essential, but so-far unreported characteristics of K5 and Z carriers. State-of-the-art process models and biofilm-reactor performance measures are

based on biofilm area, and an implemented system must provide the required biofilm area. A generally accepted design approach requires a model user to define specific surface area (SSA) and displacement for 1-m^3 of carriers, which is analogous to 100% carrier fill when considering a 1-m^3 bioreactor. For example, K5 has 800 m_F^2/m_C^3 SSA. For Z-carriers, SSA and displacement is expressed in terms of the number of pieces. Information such as m^2/mp, kg/mp, and approximate m^3/mp is needed for process design and cost estimation. **Table 25** summarizes critical values for each type of plastic carrier such as mass-based plastic carrier specific surface area, displacement, and volume. **Table 25** also summarizes important conversion factors between number of carriers to mass and volume. These values now make it possible to compute the correct amount of K5 and Z carriers to include in an AnBfMBR.

Table 25. Critical Values and Important Conversions

Carrier Type	Mass (g)	SSA (m_F^2/kg)	Di (m_W^3/m_C^3)	Volume (kg/m_C^3)	Volume (#/m_C^3)	Volume of Liquid Displaced (m_W^3/#)
K5	0.36	7.2	0.19	114	314,000	6×10^{-7}
Z-200	0.37	4.1	0.24	223	604,000	4×10^{-7}
Z-400	0.38	4.0	0.25	232	614,000	4×10^{-7}

Other objectives of this thesis project were: 1) systematically evaluate how the mixed-liquor suspended solids (MLSS) controls the permeate flux through the ceramic membranes; 2) document the impact of biofilm carriers on mitigating membrane fouling and the build up of transmembrane pressure (TMP) for a relevant range of MLSS concentrations and carrier-fill ratios; and 3) evaluate the impact of power input on biofilm carrier membrane mixing and scouring efficiency. In Chapter 4, I carried out series of permeate-flux experiments with K5 and Z-400 carriers with the aim to achieve

the objectives. The experiments revealed two distinct trends. First, the time to failure TMP decreased as MLSS concentration increased. Second, increasing the carrier fill extend the time to failure, particularly for higher MLSS concentrations. Taken together, the experiments identified an optimized "sweet spot" for the AnBfMBR: e.g., an operating flux of 0.25-m/d, a failure TMP of 0.3-atm pressure, MLSS of 5,000 – 7,500 mg/L, and 40% carrier fill for the Z-400 carriers.

5.2. Recommendations

This thesis project resulted in important science, technology, and engineering outcomes that make it possible to complete design of an optimized AnBfMBR system. In this section, I provide several recommendations for future work conducting experiments with the bench-scale AnBfMBR.

My first recommendation is to focus on the interactions of the plastic biofilm carriers and the ceramic membranes. I specifically suggest evaluating the long-term impact of biofilm carriers on membrane integrity. According to Shin and Bae (2018), who did extensive work on the SAF-MBR, a future research need for all AnMBRs is an assessment of the sustainability of the membranes, because their experience showed that carriers could abrade the polymeric membranes and reduce membrane life. While ceramic membranes ought to be much more robust against abrasion that are polymeric membranes, long-term robustness must be evaluated. I recommend that membrane abrasion and robustness be evaluated in pilot-scale testing, since it can be operated at a longer run time (i.e., months to years) and simulates the actual physical environment better than does a bench-scale system.

My second recommendation is to identify an optimal membrane spacing and module stacking for use with K5 and Z-carriers. I was able to evaluate only one membrane-plate spacing, 60 mm, and I had only one module. Closer spacing of the membrane plates can allow more membrane area per unit volume, but the spacing must allow free movement of the carriers between the plates. Scaling the AnBfMBR from bench-scale to pilot-scale and full-scale may require alterations to the membrane configuration and membrane modules inside a reactor tank. For example, pilot-scale and full-scale systems need many modules, which requires them to be stacked. Stacking and placement of modules next to each other will require additional effort to design. Again, these module feature need to be evaluated in pilot-scale systems.

It is worth noting the limitations of my work, which stem from short-term testing with diluted AD sludge. The longest operating time was 2 hours and 46 minutes, which occurred for the Z-400 carrier experiments. Longer-term operation would lead to biofilm accumulation on the plastic carriers. Biofilm accumulation would have effects on plastic carrier density, buoyancy, and scouring of the ceramic membranes. Longer-term operation also could lead to cake build-up on the ceramic membranes, which could be positive or negative. Cake build-up could have a positive effect because it can filter and protect the membrane from fine particles, which contribute to irreversible membrane fouling. On the other hand, excessive cake build-up will lead to membrane fouling.

REFERENCES

AnMBR generates power and water for reuse from industrial wastewater. (2015). *Membrane Technology*, *2015*(1), 9–10. https://doi.org/https://doi.org/10.1016/S0958-2118(15)70019-4

Aqeel, H., Weissbrodt, D.G., Cerruti, M., Wolfaardt, G.M., Wilen, B.-M., Liss, S.N. (2019). Drivers of bioaggregation from flocs to biofilms and granular sludge. *Env. Sci. Wat. Res. Technol*. **5**. 2072-2089.

Biothane Solutions (2021). AnMBBR [Drawing]. Retrieved from https://www.biothanesolutions.com/sites/g/files/dvc4081/files/document/2021/07/Anoxthane_Brochure.pdf

Boltz, J. P., Smets, B. F., Rittmann, B. E., Van Loosdrecht, M. C., Morgenroth, E., & Daigger, G. T. (2017). From biofilm ecology to reactors: a focused review. *Water Science and Technology*, *75*(8), 1753-1760.

Daigger, G. T., & Boltz, J. P. (2018). Oxygen Transfer in Moving Bed Biofilm Reactor and Integrated Fixed Film Activated Sludge Processes. *Water Environment Research*, *90*(7), 615-622.

Dohányos, M., Zabranska, J., Kutil, J., & Jeníček, P. (2004). Improvement of anaerobic digestion of sludge. *Water Science and Technology*, *49*(10), 89-96.

Elger, D. F., LeBret, B. A., Crowe, C. T., & Roberson, J. A. (2020). *Engineering Fluid Mechanics*. John Wiley & Sons.

Gitis, V., & Rothenburg, G. (2016). Ceramic membranes: new opportunities and practical applications. *Wiley*, 1–90. https://doi.org/https://doi.org/10.1002/9783527696550.ch1

Guo, J., Guan, W., & Xia, S. (2014). Membrane fouling of hybrid submerged membrane bioreactor (hMBR) in treating municipal wastewater. *Desalination and Water Treatment*, *52*(37–39), 6858–6867. https://doi.org/10.1080/19443994.2013.831778

Hao, X., Li, J., van Loosdrecht, M. C., Jiang, H., & Liu, R. (2019). Energy recovery from wastewater: Heat over organics. *Water research*, *161*, 74-77.

Heald, C. C. (2018). *Cameron Hydraulic Data Book*. Flowserve, Texas.

Jin, L., Ong, S. L., & Ng, H. Y. (2013). Fouling control mechanism by suspended biofilm carriers addition in submerged ceramic membrane bioreactors. *Journal of Membrane Science*, *427*, 250–258. https://doi.org/10.1016/j.memsci.2012.09.016

Judd, S. (2008). The status of membrane bioreactor technology. *Trends in biotechnology*, *26*(2), 109-116.

Kim, J., Kim, K., Ye, H., Lee, E., Shin, C., McCarty, P. L., & Bae, J. (2011). Anaerobic Fluidized Bed Membrane Bioreactor for Wastewater Treatment. *Environmental Science & Technology*, *45*(2), 576–581. https://doi.org/10.1021/es1027103

Lee, W. N., Kang, I. J., & Lee, C. H. (2006). Factors affecting filtration characteristics in membrane-coupled moving bed biofilm reactor. *Water Research*, *40*(9), 1827–1835. https://doi.org/10.1016/j.watres.2006.03.007

Maaz, M., Yasin, M., Aslam, M., Kumar, G., Atabani, A. E., Idrees, M., ... & Kim, J. (2019). Anaerobic membrane bioreactors for wastewater treatment: Novel configurations, fouling control and energy considerations. *Bioresource technology*, *283*, 358-372.

McQuarrie, J. P., & Boltz, J. P. (2011). Moving bed biofilm reactor technology: process applications, design, and performance. *Water Environment Research*, *83*(6), 560–575. https://doi.org/10.2175/106143010x12851009156286

Milnes, M. The Mathematics of Pumping Water AECOM Design Build Civil. *Mechanical Engineering. The Royal Academy of Engineering. Retrieved from http://www. raeng. org. uk/publications/other/17-pumping-water*.

Pang, C., Ren, X., Zhang, X., Hu, Z., & Wang, W. (2020). Influence of immersion depth of membrane on filtration performance of anaerobic membrane bioreactor. *Environmental Science and Pollution Research*, *27*(23), 29433–29440. https://doi.org/10.1007/s11356-020-09213-1

PAQUES (2021). BIOPAQ IC [Drawing]. Retrieved from https://en.paques.nl/products/featured/biopaq-anaerobic-wastewater-treatment/biopaqic

Parkin, G. F., & Owen, W. F. (1986). Fundamentals of anaerobic digestion of wastewater sludges. *Journal of environmental engineering*, *112*(5), 867-920.

Rittmann, B. E., & McCarty, P. L. (2001). *Environmental Biotechnology: Principles and Applications* (1st ed.). New York: McGraw-Hill.

Rittmann, B. E., & McCarty, P. L. (2020). *Environmental Biotechnology: Principles and Applications* (2nd ed.). New York: McGraw-Hill.

SafBon Water (2021). Ceramic Ultrafiltration, CFM Systems [Drawing]. Retrieved from https://www.safbonwater.com/ceramic-ultrafiltration-2/

Shin, C., Kim, K., McCarty, P. L., Kim, J., & Bae, J. (2016). Integrity of hollow-fiber membranes in a pilot-scale anaerobic fluidized membrane bioreactor (AFMBR) after two-years of operation. *Separation and Purification Technology*, *162*, 101–105. https://doi.org/10.1016/j.seppur.2016.02.019

Shin, C., & Bae, J. (2018). Current status of the pilot-scale anaerobic membrane bioreactor treatments of domestic wastewaters: A critical review. *Bioresource technology*, *247*, 1038-1046.

Smith, A. L., Stadler, L. B., Love, N. G., Skerlos, S. J., & Raskin, L. (2012). Perspectives on anaerobic membrane bioreactor treatment of domestic wastewater: a critical review. *Bioresource technology*, *122*, 149-159.

Smith, A. L., Stadler, L. B., Cao, L., Love, N. G., Raskin, L., & Skerlos, S. J. (2014). Navigating wastewater energy recovery strategies: a life cycle comparison of anaerobic membrane bioreactor and conventional treatment systems with anaerobic digestion. *Environmental science & technology*, *48*(10), 5972-5981.

Suez Water Technologies (2021). Anaerobic MBR Technology [Drawing]. Retrieved from https://www.suezwatertechnologies.com/products/biowaste/anaerobic-mbr

Uni-Bell PVC Pipe Association, 2012 (5th ed.). *Handbook of PVC Pipe Design and Construction*. Uni-Bell PVC Pipe Association, Dallas, Texas

APPENDIX A

POWER INPUT AND VELOCITY GRADIENT CALCULATIONS FOR A FLOW RATE OF 10 GPM

Table A1. Solving for the Friction Factor Using the Colebrook Equation (For Total Flow)

Row #	Properties	English Units	SI Units	Reference (as relevant)
1	Density of Water (10˚C)	62.4 lbm/ft^3	1000 kg/m^3	Elger et al., 2020
2	Dynamic Viscosity of Water (10˚C)	0.00088 lbm/(ft-s)	0.00131 Pa·s	Elger et al., 2020
3	Gravity	32.2 lbm ft/s^2	9.8 m/s^2	Elger et al., 2020
4	Pipe Diameter	0.083 ft	0.025 m	-
5	Cross Sectional Area	0.005 ft^2	0.0005 m^2	-
6	Total Pipe Length	7.83 ft	2.4 m	-
7	Volumetric Flow Rate	0.022 ft^3/s	0.0006 m^3/s	-
8	Average Velocity (Volumetric Flow Rate/Cross Sectional Area)	4.1 ft/s	1.2 m/s	-
9	Reynolds Number **(**Equation 5**)**	23,943	-	-
10	Pipe Roughness (PVC Pipe)	0.0000049 ft	0.0021 mm	Uni-Bell, 2012
11	Relative Roughness	5.9E-05	-	-
12	Friction Factor	0.024	-	-
13	LHS of Colebrook Equation	6.33	-	-
14	RHS of Colebrook Equation	6.33	-	-
15	Difference	0	-	-
16	Squared Difference	0	-	-

Table A2. Solving for the Friction Factor Using the Colebrook Equation (For 1/4th Total Flow)

Row #	Properties	English Units	SI Units	Reference (as relevant)
1	Density of Water (20 C)	62.4 lbm/ft^3	1000 kg/m^3	Elger et al., 2020
2	Dynamic Viscosity of Water (20 C)	0.00088 lbm/(ft-s)	0.00131 Pa·s	Elger et al., 2020
3	Gravity	32.2 lbm ft/s^2	9.8 m/s^2	Elger et al., 2020
4	Pipe Diameter	0.083 ft	0.025 m	-
5	Cross Sectional Area	0.005 ft^2	0.0005 m^2	-
6	Total Pipe Length	0.5 ft	0.15 m	-
7	Volumetric Flow Rate	0.006 ft^3/s	0.0002 m^3/s	-
8	Average Velocity (Volumetric Flow Rate/Cross Sectional Area)	1.0 ft/s	0.3 m/s	-
9	Reynolds Number (Equation 5)	5,896	-	-
10	Pipe Roughness (PVC Pipe)	0.0000049 ft	0.0021 mm	Uni-Bell, 2012
11	Relative Roughness	5.9E-05	-	-
12	Friction Factor	0.036	-	-
13	LHS of Colebrook Equation	5.3	-	-
14	RHS of Colebrook Equation	5.3	-	-
15	Difference	0	-	-
16	Squared Difference	0	-	-

For total flow:

$$h_{major} = 0.025 \cdot \left(\frac{7.83 \text{ ft}}{0.083 \text{ ft}}\right) \cdot \left(\frac{(4.1 \text{ ft/s})^2}{2 \cdot 32.2 \text{ ft/s}^2}\right) = 0.62 \text{ ft}$$

Major Head Loss = 0.62 ft

For 1/4th flow:

$$h_{major} = 0.036 \cdot \left(\frac{0.5 \text{ ft}}{0.083 \text{ ft}}\right) \cdot \left(\frac{\left(1.0 \frac{\text{ft}}{\text{s}}\right)^2}{2 \cdot 32.2 \frac{\text{ft}}{\text{s}^2}}\right) = 0.003 \text{ ft}$$

Major Head Loss = 0.003 ft

Total Major Head Loss = 0.62 ft + 0.003 ft = 0.623 ft = 0.2 m

For total flow:

$$h_{minor} = \frac{(4.1\ ft/s)^2}{2 \cdot 32.2\ ft/s^2} \cdot 8.29$$

$$h_{minor} = 2.16\ ft\ \ (0.66\ m)$$

For 1/4th flow:

$$h_{minor} = \frac{(1.0\ ft/s)^2}{2 \cdot 32.2\ ft/s^2} \cdot 6.86$$

$$h_{minor} = 0.11\ ft\ (0.03\ m)$$

Total Minor Head Loss = 2.16 ft + 0.11 ft = 2.27 ft = 0.69 m

Minor head loss – orifice:

$$2.5\ GPM = 19.636 \cdot 0.96 \cdot 0.3125\ in^2 \cdot \sqrt{h}$$

$$h = 1.84\ ft\ (0.56\ m)$$

Table A3. Summary of Head Losses

Static Head Loss	0.88 ft (0.27 m)
Major Head Loss	0.623 ft (0.20 m)
Minor Head Loss	2.27 ft (0.69 m)
Orifice Head Loss	1.84 ft (0.56 m)

Total System Head = Static Head + Major Head + Minor Head + Orifice Head

= 0.88 ft + 0.623 ft + 2.27 ft + 1.84 ft = 5.61 ft = 1.71 m

$P = \gamma \cdot Q \cdot H = (9{,}810\ N/m^3) \cdot (0.0006\ m^3/s) \cdot (1.71\ m) = 10\ W$ or 91

W/m^3

$$G = \sqrt{P / \mu \cdot V} = \sqrt{10\ W/(1.31 \times 10^{-3}\ N \cdot s/m^2 \cdot 0.08\ m^3)} = 308\ 1/s$$

APPENDIX B

POWER INPUT AND VELOCITY GRADIENT CALCULATIONS FOR A FLOW RATE OF 9 GPM

Table B1. Solving for the Friction Factor Using the Colebrook Equation (For Total Flow)

Row #	Properties	English Units	SI Units	Reference (as relevant)
1	Density of Water (10˚C)	62.4 lbm/ft^3	1000 kg/m^3	Elger et al., 2020
2	Dynamic Viscosity of Water (10˚C)	0.00088 lbm/(ft-s)	0.00131 Pa·s	Elger et al., 2020
3	Gravity	32.2 lbm ft/s^2	9.8 m/s^2	Elger et al., 2020
4	Pipe Diameter	0.083 ft	0.025 m	-
5	Cross Sectional Area	0.005 ft^2	0.0005 m^2	-
6	Total Pipe Length	7.83 ft	2.4 m	-
7	Volumetric Flow Rate	0.02 ft^3/s	0.0006 m^3/s	-
8	Average Velocity (Volumetric Flow Rate/Cross Sectional Area)	3.7 ft/s	1.1 m/s	-
9	Reynolds Number (Equation 5)	21,766	-	-
10	Pipe Roughness (PVC Pipe)	0.0000049 ft	0.0021 mm	Uni-Bell, 2012
11	Relative Roughness	5.9E-05	-	-
12	Friction Factor	0.025	-	-
13	LHS of Colebrook Equation	6.26	-	-
14	RHS of Colebrook Equation	6.26	-	-
15	Difference	0	-	-
16	Squared Difference	0	-	-

Table B2. Solving for the Friction Factor Using the Colebrook Equation (For 1/4th Total Flow)

Row #	Properties	English Units	SI Units	Reference (as relevant)
1	Density of Water (20 C)	62.4 lbm/ft^3	1000 kg/m^3	Elger et al., 2020
2	Dynamic Viscosity of Water (20 C)	0.00088 lbm/(ft-s)	0.00131 Pa·s	Elger et al., 2020
3	Gravity	32.2 lbm ft/s^2	9.8 m/s^2	Elger et al., 2020
4	Pipe Diameter	0.083 ft	0.025 m	-
5	Cross Sectional Area	0.005 ft^2	0.0005 m^2	-
6	Total Pipe Length	0.5 ft	0.15 m	-
7	Volumetric Flow Rate	0.005 ft^3/s	0.0001 m^3/s	-
8	Average Velocity (Volumetric Flow Rate/Cross Sectional Area)	0.9 ft/s	0.3 m/s	-
9	Reynolds Number (Equation 5)	5,442	-	-
10	Pipe Roughness (PVC Pipe)	0.0000049 ft	0.0021 mm	Uni-Bell, 2012
11	Relative Roughness	5.9E-05	-	-
12	Friction Factor	0.037	-	-
13	LHS of Colebrook Equation	5.23	-	-
14	RHS of Colebrook Equation	5.3	-	-
15	Difference	0	-	-
16	Squared Difference	0	-	-

For total flow:

$$h_{major} = 0.025 \cdot \left(\frac{7.83 \text{ ft}}{0.083 \text{ ft}}\right) \cdot \left(\frac{(3.7 \text{ ft/s})^2}{2 \cdot 32.2 \text{ ft/s}^2}\right) = 0.51 \text{ ft}$$

Major Head Loss = 0.51 ft

For 1/4th flow:

$$h_{major} = 0.037 \cdot \left(\frac{0.5 \text{ ft}}{0.083 \text{ ft}}\right) \cdot \left(\frac{\left(0.9 \frac{\text{ft}}{\text{s}}\right)^2}{2 \cdot 32.2 \frac{\text{ft}}{\text{s}^2}}\right) = 0.003 \text{ ft}$$

Major Head Loss = 0.003 ft

Total Major Head Loss = 0.51 ft + 0.003 ft = 0.513 ft = 0.16 m

For total flow:

$$h_{minor} = \frac{(3.7\ ft/s)^2}{2 \cdot 32.2\ ft/s^2} \cdot 8.29$$
$$h_{minor} = 1.8\ ft\ \ (0.54\ m)$$

For 1/4th flow:

$$h_{minor} = \frac{(0.9\ ft/s)^2}{2 \cdot 32.2\ ft/s^2} \cdot 6.86$$
$$h_{minor} = 0.09\ ft\ (0.03\ m)$$

Total Minor Head Loss = 1.8 ft + 0.09 ft = 1.89 ft = 0.58 m

Minor head loss – orifice:

$$2.25\ GPM = 19.636 \cdot 0.96 \cdot 0.3125\ in^2 \cdot \sqrt{h}$$
$$h = 1.49\ ft\ (0.45\ m)$$

Table B3. Summary of Head Losses

Static Head Loss	0.88 ft (0.27 m)
Major Head Loss	0.513 ft (0.16 m)
Minor Head Loss	1.89 ft (0.58 m)
Orifice Head Loss	1.49 ft (0.45 m)

Total System Head = Static Head + Major Head + Minor Head + Orifice Head

= 0.88 ft + 0.513 ft + 1.89 ft + 1.49 ft = 4.77 ft = 1.5 m

$$P = \gamma \cdot Q \cdot H = (9{,}810\ N/m^3) \cdot (0.0006\ m^3/s) \cdot (1.5\ m) = 9\ W \text{ or } 80\ W/m^3$$

$$G = \sqrt{P / \mu \cdot V} = \sqrt{9\ W/(1.31 \times 10^{-3}\ N \cdot s/m^2 \cdot 0.08\ m^3)} = 293\ 1/s$$

APPENDIX C

POWER INPUT AND VELOCITY GRADIENT CALCULATIONS FOR A FLOW RATE OF 8 GPM

Table C1. Solving for the Friction Factor Using the Colebrook Equation (For Total Flow)

Row #	Properties	English Units	SI Units	Reference (as relevant)
1	Density of Water (10˚C)	62.4 lbm/ft^3	1000 kg/m^3	Elger et al., 2020
2	Dynamic Viscosity of Water (10˚C)	0.00088 lbm/(ft-s)	0.00131 Pa·s	Elger et al., 2020
3	Gravity	32.2 lbm ft/s^2	9.8 m/s^2	Elger et al., 2020
4	Pipe Diameter	0.083 ft	0.025 m	-
5	Cross Sectional Area	0.005 ft^2	0.0005 m^2	-
6	Total Pipe Length	7.83 ft	2.4 m	-
7	Volumetric Flow Rate	0.018 ft^3/s	0.0005 m^3/s	-
8	Average Velocity (Volumetric Flow Rate/Cross Sectional Area)	3.3 ft/s	1.0 m/s	-
9	Reynolds Number (Equation 5)	19,590	-	-
10	Pipe Roughness (PVC Pipe)	0.0000049 ft	0.0021 mm	Uni-Bell, 2012
11	Relative Roughness	5.9E-05	-	-
12	Friction Factor	0.026	-	-
13	LHS of Colebrook Equation	6.18	-	-
14	RHS of Colebrook Equation	6.18	-	-
15	Difference	0	-	-
16	Squared Difference	0	-	-

Table C2. Solving for the Friction Factor Using the Colebrook Equation (For 1/4th Total Flow)

Row #	Properties	English Units	SI Units	Reference (as relevant)
1	Density of Water (20 C)	62.4 lbm/ft^3	1000 kg/m^3	Elger et al., 2020
2	Dynamic Viscosity of Water (20 C)	0.00088 lbm/(ft-s)	0.00131 Pa·s	Elger et al., 2020
3	Gravity	32.2 lbm ft/s^2	9.8 m/s^2	Elger et al., 2020
4	Pipe Diameter	0.083 ft	0.025 m	-
5	Cross Sectional Area	0.005 ft^2	0.0005 m^2	-
6	Total Pipe Length	0.5 ft	0.15 m	-
7	Volumetric Flow Rate	0.0045 ft^3/s	0.0001 m^3/s	-
8	Average Velocity (Volumetric Flow Rate/Cross Sectional Area)	0.8 ft/s	0.2 m/s	-
9	Reynolds Number (Equation 5)	4,897	-	-
10	Pipe Roughness (PVC Pipe)	0.0000049 ft	0.0021 mm	Uni-Bell, 2012
11	Relative Roughness	5.9E-05	-	-
12	Friction Factor	0.038	-	-
13	LHS of Colebrook Equation	5.2	-	-
14	RHS of Colebrook Equation	5.2	-	-
15	Difference	0	-	-
16	Squared Difference	0	-	-

For total flow:

$$h_{major} = 0.026 \cdot \left(\frac{7.83 \text{ ft}}{0.083 \text{ ft}}\right) \cdot \left(\frac{(3.3 \text{ ft/s})^2}{2 \cdot 32.2 \text{ ft/s}^2}\right) = 0.41 \text{ ft}$$

Major Head Loss = 0.41 ft

For 1/4th flow:

$$h_{major} = 0.038 \cdot \left(\frac{0.5 \text{ ft}}{0.083 \text{ ft}}\right) \cdot \left(\frac{\left(0.8 \frac{\text{ft}}{\text{s}}\right)^2}{2 \cdot 32.2 \frac{\text{ft}}{\text{s}^2}}\right) = 0.002 \text{ ft}$$

Major Head Loss = 0.002 ft

Total Major Head Loss = 0.41 ft + 0.002 ft = 0.412 ft = 0.1 m

For total flow:

$$h_{minor} = \frac{(3.3\ ft/s)^2}{2 \cdot 32.2\ ft/s^2} \cdot 8.29$$
$$h_{minor} = 1.4\ ft\ \ (0.43\ m)$$

For 1/4th flow:

$$h_{minor} = \frac{(0.8\ ft/s)^2}{2 \cdot 32.2\ ft/s^2} \cdot 6.86$$
$$h_{minor} = 0.07\ ft\ (0.02\ m)$$

Total Minor Head Loss = 1.4 ft + 0.07 ft = 1.47 ft = 0.45 m

Minor head loss – orifice:

$$2\ GPM = 19.636 \cdot 0.96 \cdot 0.3125\ in^2 \cdot \sqrt{h}$$
$$h = 1.18\ ft\ (0.36\ m)$$

Table C3. Summary of Head Losses

Static Head Loss	0.88 ft (0.27 m)
Major Head Loss	0.412 ft (0.10 m)
Minor Head Loss	1.47 ft (0.45 m)
Orifice Head Loss	1.18 ft (0.36 m)

Total System Head = Static Head + Major Head + Minor Head + Orifice Head

= 0.88 ft + 0.412 ft + 1.47 ft + 1.18 ft = 3.94 ft = 1.2 m

$$P = \gamma \cdot Q \cdot H = (9{,}810\ N/m^3) \cdot (0.0005\ m^3/s) \cdot (1.2\ m) = 6\ W \text{ or } 55\ W/m^3$$

$$G = \sqrt{P / \mu \cdot V} = \sqrt{6\ W/(1.31 \times 10^{-3}\ N \cdot s/m^2 \cdot 0.08\ m^3)} = 239\ 1/s$$

APPENDIX D

CALCULATIONS OF POWER INPUT AND VELOCITY GRADIENT ASSUMING THAT ONLY STATIC HEAD IS RELEVANT

For 10 GPM:

$$P = \gamma \cdot Q \cdot H = (9{,}810\ N/m^3) \cdot (0.0006\ m^3/s) \cdot (0.27\ m) = 1.6\ W \text{ or } 20\ W/m^3$$

$$G = \sqrt{P / \mu \cdot V} = \sqrt{1.6\ W/(1.31 \times 10^{-3}\ N \cdot s/m^2 \cdot 0.08\ m^3)} = 124\ 1/s$$

For 9 GPM:

$$P = \gamma \cdot Q \cdot H = (9{,}810\ N/m^3) \cdot (0.00057\ m^3/s) \cdot (0.27\ m) = 1.5\ W \text{ or } 19\ W/m^3$$

$$G = \sqrt{P / \mu \cdot V} = \sqrt{1.5\ W/(1.31 \times 10^{-3}\ N \cdot s/m^2 \cdot 0.08\ m^3)} = 120\ 1/s$$

For 8 GPM:

$$P = \gamma \cdot Q \cdot H = (9{,}810\ N/m^3) \cdot (0.0005\ m^3/s) \cdot (0.27\ m) = 1.3\ W \text{ or } 16\ W/m^3$$

$$G = \sqrt{P / \mu \cdot V} = \sqrt{1.3\ W/(1.31 \times 10^{-3}\ N \cdot s/m^2 \cdot 0.08\ m^3)} = 111\ 1/s$$

APPENDIX E

CALCULATIONS OF POWER INPUT AND VELOCITY GRADIENT ASSUMING THAT BOTH THE STATIC HEAD AND ORIFICE LOSS IS RELEVANT

For 10 GPM:

$$P = \gamma \cdot Q \cdot H = (9{,}810\ N/m^3) \cdot (0.0006\ m^3/s) \cdot (0.27 + 0.56\ m) = 6\ W \text{ or } 61\ W/m^3$$

$$G = \sqrt{P / \mu \cdot V} = \sqrt{6\ W/(1.31 \times 10^{-3}\ N \cdot s/m^2 \cdot 0.08\ m^3)} = 239\ 1/s$$

For 9 GPM:

$$P = \gamma \cdot Q \cdot H = (9{,}810\ N/m^3) \cdot (0.00057\ m^3/s) \cdot (0.27 + 0.45\ m) = 4\ W \text{ or } 50\ W/m^3$$

$$G = \sqrt{P / \mu \cdot V} = \sqrt{4\ W/(1.31 \times 10^{-3}\ N \cdot s/m^2 \cdot 0.08\ m^3)} = 195\ 1/s$$

For 8 GPM:

$$P = \gamma \cdot Q \cdot H = (9{,}810\ N/m^3) \cdot (0.0005\ m^3/s) \cdot (0.27 + 0.36\ m) = 3\ W \text{ or } 39\ W/m^3$$

$$G = \sqrt{P / \mu \cdot V} = 169\ 1/s$$

APPENDIX F

MASS MEASUREMENTS

Table F1. Mass Measurements of K5 Carriers

Number of K5	Mass Measure 1 (g)	Mass Measure 2 (g)	Mass Measure 3 (g)	Average Mass (g)	Minimum Mass (g)	Maximum Mass (g)	Standard Deviation
0	0	0	0	0	0	0	0
50	18.4	18.4	18.4	18.4	18.4	18.4	0
250	90.9	90.9	90.9	90.9	90.9	90.9	1.74×10^{-14}
500	182	182	182	182	182	182	3.48×10^{-14}
1,000	362	362	362	362	362	362	0

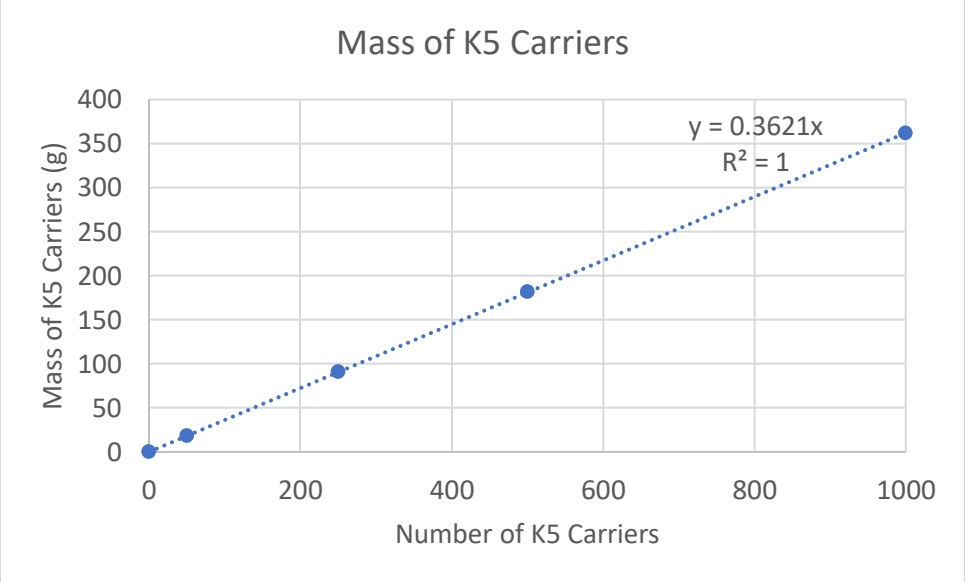

Figure F1. Mass of K5 Carriers (Slope = 0.3621 g/#)

Table F2. Mass Measurements of Z-200 Carriers

Number of Z-200	Mass Measure 1 (g)	Mass Measure 2 (g)	Mass Measure 3 (g)	Average Mass (g)	Minimum Mass (g)	Maximum Mass (g)	Standard Deviation
0	0	0	0	0	0	0	0
50	18.7	18.7	18.7	18.7	18.7	18.7	0
250	93	93.1	93.1	93.1	93	93.1	0.058
500	179	179	179	179	179	179	0
1,000	371	3701	371	3701	371	371	0.058

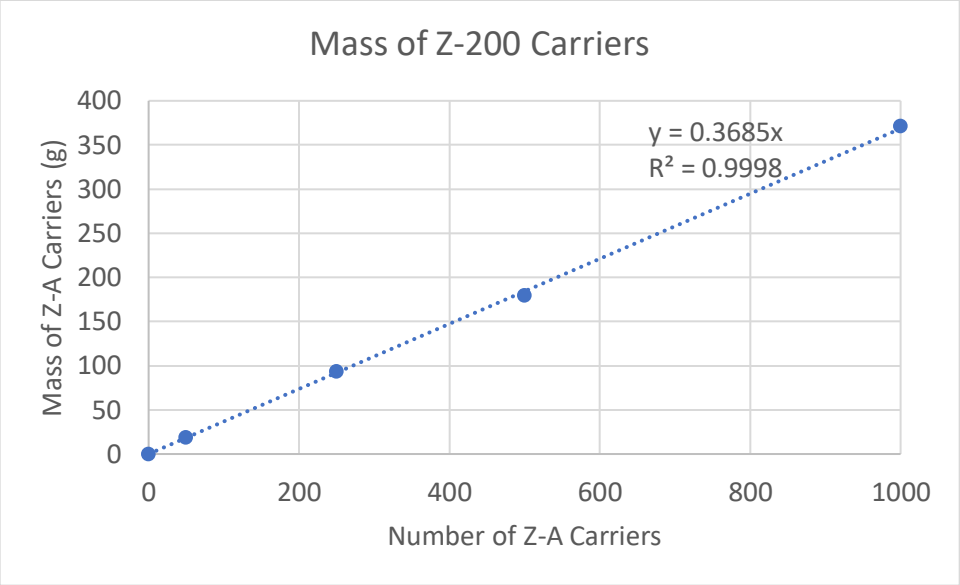

Figure F2. Mass of Z-200 Carriers (Slope = 0.3685 g/#)

Table F3. Mass Measurements of Z-400 Carriers

Number of Z-400	Mass 1 (g)	Mass 2 (g)	Mass 3 (g)	Average Mass (g)	Minimum Mass (g)	Maximum Mass (g)	Standard Deviation
0	0	0	0	0	0	0	0
50	20	20	20	20	20	20	0
250	93.7	93.7	93.7	93.7	93.7	93.7	0
500	188	188	188	188	188	188	0.058
1,000	378	378	378	378	378	378	0.058

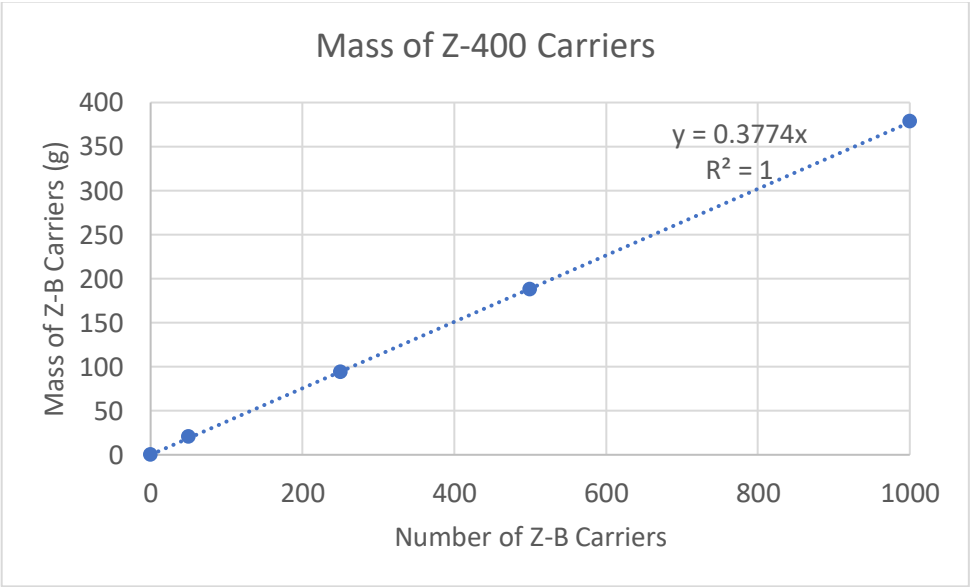

Figure F3. Mass of Z-400 Carriers (Slope = 0.3774 g/#)

APPENDIX G

VOLUME MEASUREMENTS

Table G1. Volume Measurements of K5 Carriers

Volume of Container (mL)	Mass of Container (g)	Total Mass, Container + Carriers (g)	Mass of Carriers (g)	Number of Carriers
0	0	0	0	0
710	21.1	106	84.7	234
946	28.6	132	103	285
1890	44.6	260	215	594

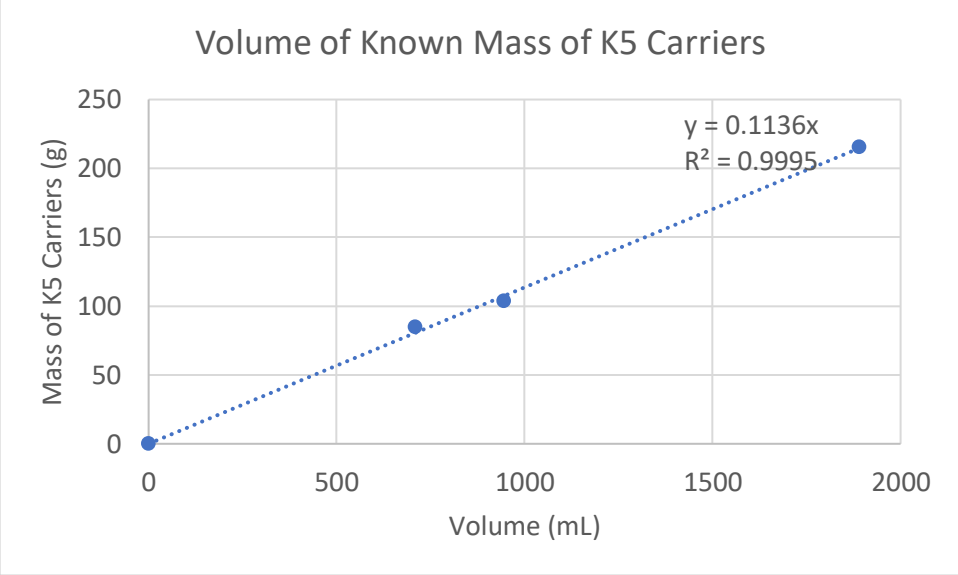

Figure G1. Volume of K5 Carriers (Mass) (Slope = 0.1136 g/mL)

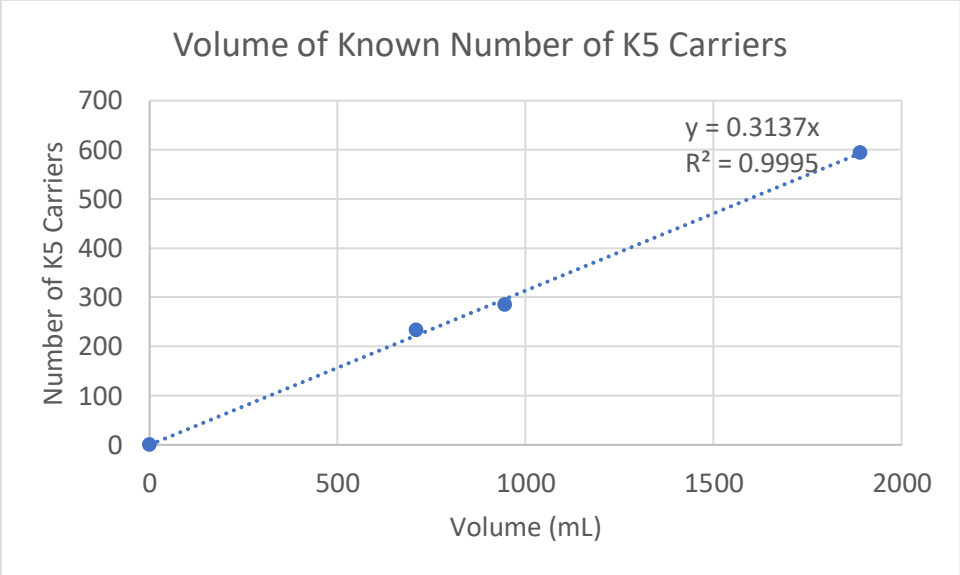

Figure G2. Volume of K5 Carriers (Carrier Count) (Slope = 0.3137 #/mL)

Table G2. Volume Measurements of Z-200 Carriers

Volume of Container (mL)	Mass of Container (g)	Total Mass, Container + Carriers (g)	Mass of Carriers (g)	Number of Carriers
0	0	0	0	0
710	21.1	182	161	437
946	28.6	242	213	578
1890	44.6	463	419	1136

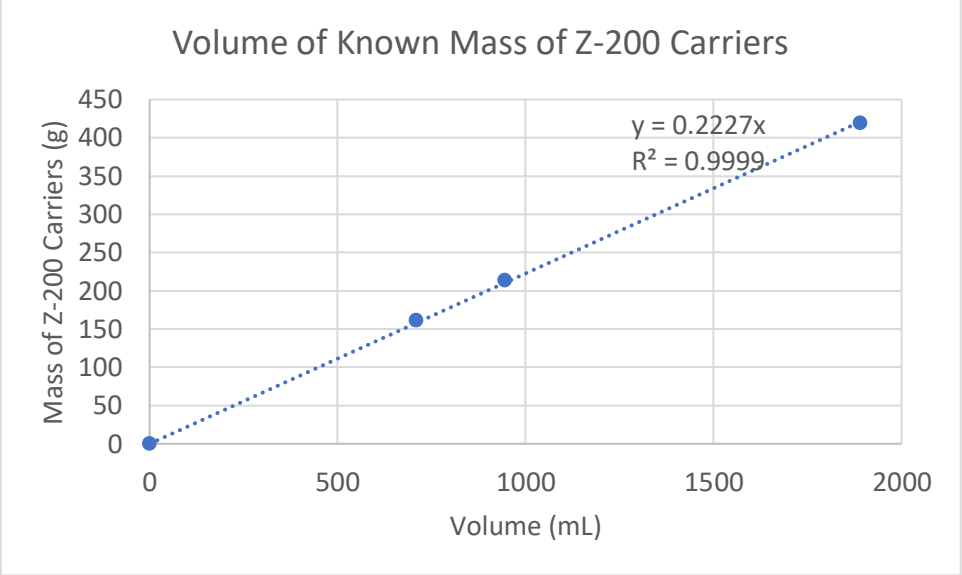

Figure G3. Volume of Z-200 Carriers (Mass) (Slope = 0.2227 g/mL)

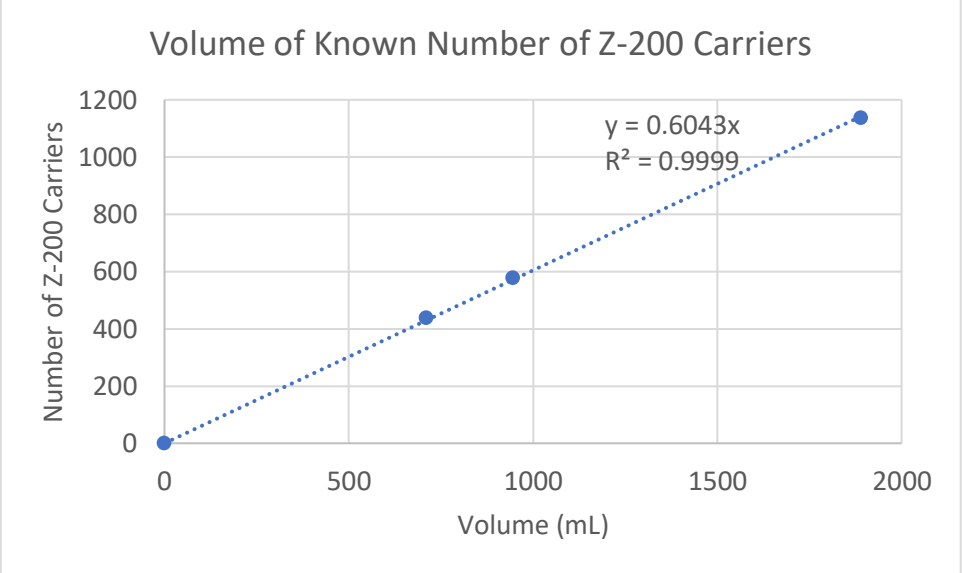

Figure G4. Volume of Z-200 Carriers (Carrier Count) (Slope = 0.6043 #/mL)

Table G3. Volume Measurements of Z-400 Carriers

Volume of Container (mL)	Mass of Container (g)	Total Mass, Container + Carriers (g)	Mass of Carriers (g)	Number of Carriers
0	0	0	0	0
710	21.1	193	172	457
946	28.6	268	239	634
1890	44.6	469	425	1126

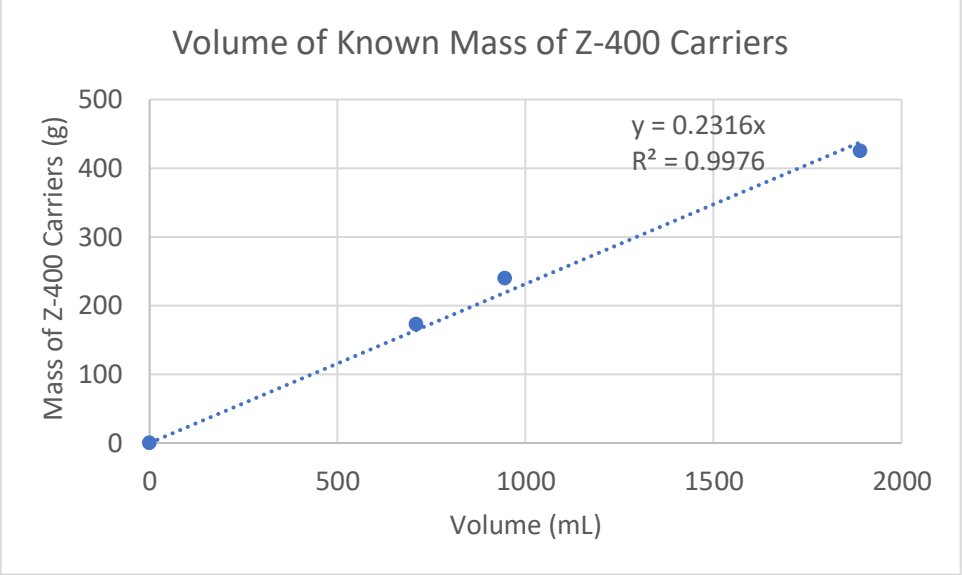

Figure G5. Volume of Z-400 Carriers (Mass) (Slope = 0.2316 g/mL)

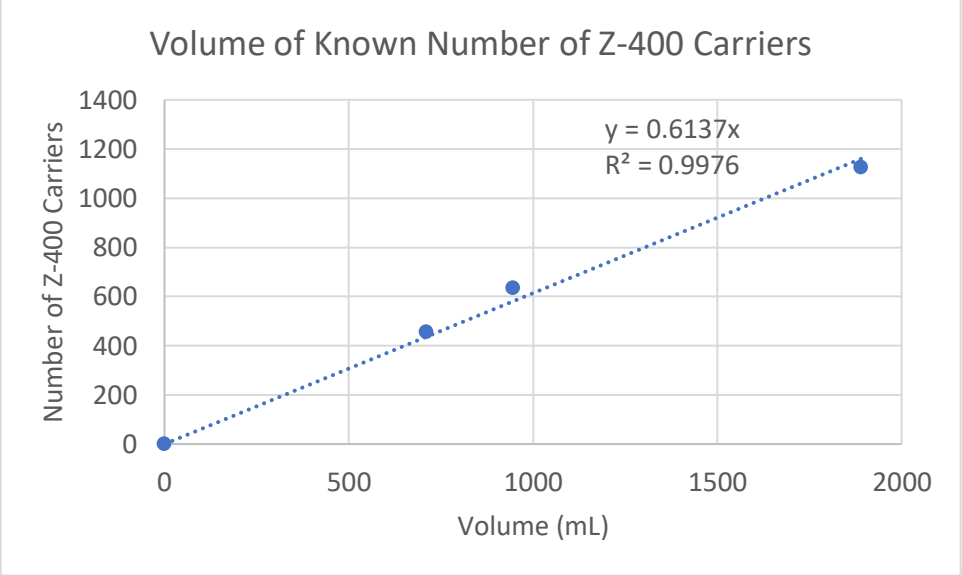

Figure G6. Volume of Z-400 Carriers (Carrier Count) (Slope = 0.6137 #/mL)

APPENDIX H

DISPLACEMENT MEASUREMENTS

Table H1. Displacement Measurements of K5 Carriers

Number of K5	Average Water EL (m)	Volume of Liquid Displaced (m_C^3)	Ratio of Volume of Liquid Displaced to Total Water Volume (m3/m3, %)
0	0	0	0
50	5×10^{-4}	1.91×10^{-5}	0.24
250	5×10^{-3}	1.91×10^{-4}	2.39
500	9×10^{-3}	3.44×10^{-4}	4.30
1,000	1.4×10^{-2}	5.36×10^{-4}	6.69

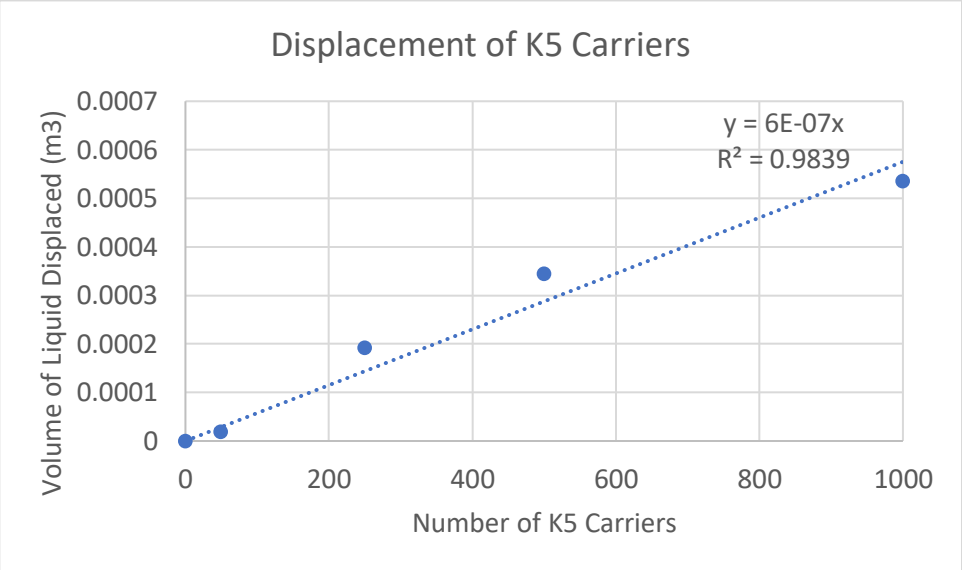

Figure H1. Displacement of K5 Carriers

Table H2. Displacement Measurements of Z-200 Carriers

Number of Z-200	Average Water EL (m)	Volume of Liquid Displaced (m_C^3)	Ratio of Volume of Liquid Displaced to Total Water Volume
0	0	0	0
50	1×10^{-5}	3.83×10^{-7}	0.005
250	3×10^{-3}	1.15×10^{-4}	1.43
500	6×10^{-3}	2.30×10^{-4}	2.87
1,000	1.1×10^{-2}	4.21×10^{-4}	5.26

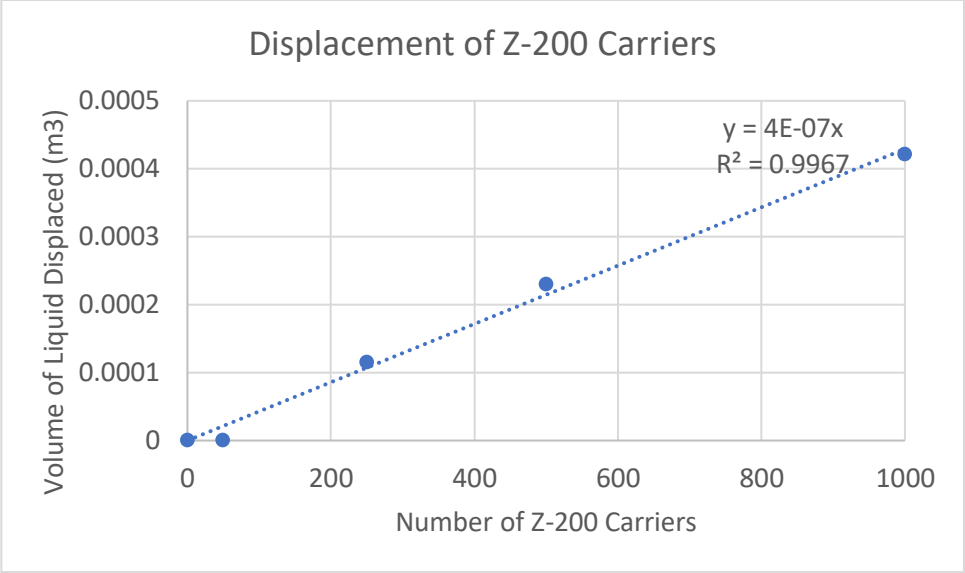

Figure H2. Displacement of Z-200 Carriers

Table H3. Displacement Measurements of Z-400 Carriers

Number of Z-400	**Average Water EL (m)**	**Volume of Liquid Displaced (m_C^3)**	**Ratio of Volume of Liquid Displaced to Total Water Volume**
0	0	0	0
50	1×10^{-5}	3.83×10^{-7}	0.005
250	2×10^{-3}	7.70×10^{-5}	0.96
500	6×10^{-3}	2.30×10^{-4}	2.87
1,000	1.1×10^{-2}	4.21×10^{-4}	5.26

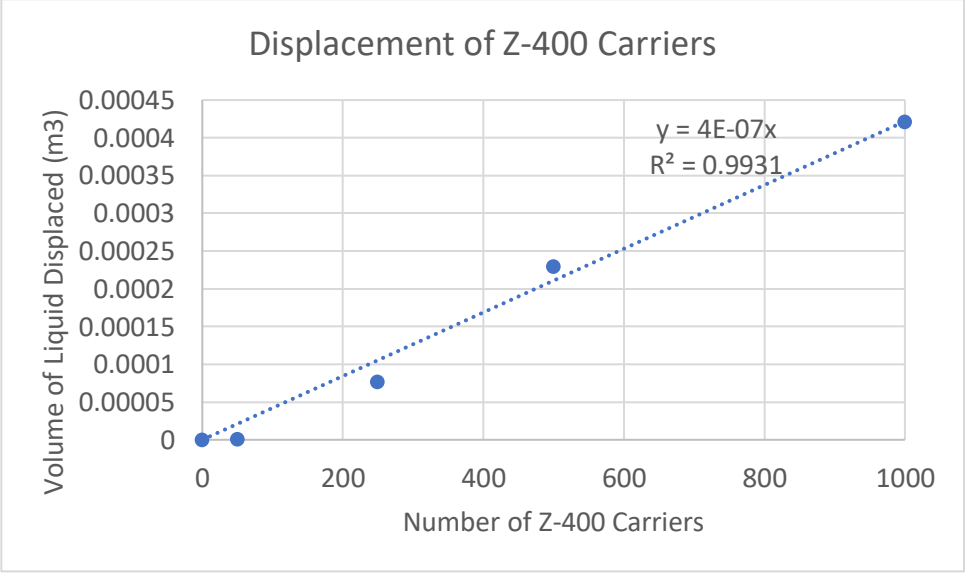

Figure H3. Displacement of Z-400 Carriers

APPENDIX I

DISPLACEMENTS FOR EXPERIMENTS RANGING FROM 0% TO 100% FILL

Table I1. K5 Carriers – Displacement Ranging from 0% to 100% Fill

Percent Fill (%)	Total Water Volume (m3)	Actual Water Volume (m3)	Number of K5 Pieces	Mass of K5 Pieces (g)	Volume of Liquid Displaced (m3)	Ratio of Volume of Liquid Displaced to Total Water Volume	Volume Occupied by K5 (m3)
0	0.08	0	0	0	0.0000	0.000	0.000
1	0.08	0.0008	251	91	0.0002	0.002	0.001
2	0.08	0.0016	502	182	0.0003	0.004	0.002
3	0.08	0.0024	754	274	0.0005	0.006	0.002
4	0.08	0.0032	1005	365	0.0006	0.008	0.003
5	0.08	0.0040	1256	456	0.0008	0.009	0.004
6	0.08	0.0048	1507	547	0.0009	0.011	0.005
7	0.08	0.0056	1758	638	0.0011	0.013	0.006
8	0.08	0.0064	2010	730	0.0012	0.015	0.006
9	0.08	0.0072	2261	821	0.0014	0.017	0.007
10	0.08	0.0080	2512	912	0.0015	0.019	0.008
11	0.08	0.0088	2763	1003	0.0017	0.021	0.009
12	0.08	0.0096	3014	1094	0.0018	0.023	0.010
13	0.08	0.0104	3266	1186	0.0020	0.024	0.010
14	0.08	0.0112	3517	1277	0.0021	0.026	0.011
15	0.08	0.0120	3768	1368	0.0023	0.028	0.012
16	0.08	0.0128	4019	1459	0.0024	0.030	0.013
17	0.08	0.0136	4270	1550	0.0026	0.032	0.014
18	0.08	0.0144	4522	1642	0.0027	0.034	0.014
19	0.08	0.0152	4773	1733	0.0029	0.036	0.015
20	0.08	0.0160	5024	1824	0.0030	0.038	0.016
21	0.08	0.0168	5275	1915	0.0032	0.040	0.017
22	0.08	0.0176	5526	2006	0.0033	0.041	0.018
23	0.08	0.0184	5778	2098	0.0035	0.043	0.018
24	0.08	0.0192	6029	2189	0.0036	0.045	0.019
25	0.08	0.0200	6280	2280	0.0038	0.047	0.020
26	0.08	0.0208	6531	2371	0.0039	0.049	0.021
27	0.08	0.0216	6782	2462	0.0041	0.051	0.022
28	0.08	0.0224	7034	2554	0.0042	0.053	0.022
29	0.08	0.0232	7285	2645	0.0044	0.055	0.023
30	0.08	0.0240	7536	2736	0.0045	0.057	0.024
31	0.08	0.0248	7787	2827	0.0047	0.058	0.025
32	0.08	0.0256	8038	2918	0.0048	0.060	0.026

33	0.08	0.0264	8290	3010	0.0050	0.062	0.026
34	0.08	0.0272	8541	3101	0.0051	0.064	0.027
35	0.08	0.0280	8792	3192	0.0053	0.066	0.028
36	0.08	0.0288	9043	3283	0.0054	0.068	0.029
37	0.08	0.0296	9294	3374	0.0056	0.070	0.030
38	0.08	0.0304	9546	3466	0.0057	0.072	0.030
39	0.08	0.0312	9797	3557	0.0059	0.073	0.031
40	0.08	0.0320	10048	3648	0.0060	0.075	0.032
41	0.08	0.0328	10299	3739	0.0062	0.077	0.033
42	0.08	0.0336	10550	3830	0.0063	0.079	0.034
43	0.08	0.0344	10802	3922	0.0065	0.081	0.034
44	0.08	0.0352	11053	4013	0.0066	0.083	0.035
45	0.08	0.0360	11304	4104	0.0068	0.085	0.036
46	0.08	0.0368	11555	4195	0.0069	0.087	0.037
47	0.08	0.0376	11806	4286	0.0071	0.089	0.038
48	0.08	0.0384	12058	4378	0.0072	0.090	0.038
49	0.08	0.0392	12309	4469	0.0074	0.092	0.039
50	0.08	0.0400	12560	4560	0.0075	0.094	0.040
51	0.08	0.0408	12811	4651	0.0077	0.096	0.041
52	0.08	0.0416	13062	4742	0.0078	0.098	0.042
53	0.08	0.0424	13314	4834	0.0080	0.100	0.042
54	0.08	0.0432	13565	4925	0.0081	0.102	0.043
55	0.08	0.0440	13816	5016	0.0083	0.104	0.044
56	0.08	0.0448	14067	5107	0.0084	0.106	0.045
57	0.08	0.0456	14318	5198	0.0086	0.107	0.046
58	0.08	0.0464	14570	5290	0.0087	0.109	0.046
59	0.08	0.0472	14821	5381	0.0089	0.111	0.047
60	0.08	0.0480	15072	5472	0.0090	0.113	0.048
61	0.08	0.0488	15323	5563	0.0092	0.115	0.049
62	0.08	0.0496	15574	5654	0.0093	0.117	0.050
63	0.08	0.0504	15826	5746	0.0095	0.119	0.050
64	0.08	0.0512	16077	5837	0.0096	0.121	0.051
65	0.08	0.0520	16328	5928	0.0098	0.122	0.052
66	0.08	0.0528	16579	6019	0.0099	0.124	0.053
67	0.08	0.0536	16830	6110	0.0101	0.126	0.054
68	0.08	0.0544	17082	6202	0.0102	0.128	0.054
69	0.08	0.0552	17333	6293	0.0104	0.130	0.055
70	0.08	0.0560	17584	6384	0.0106	0.132	0.056

71	0.08	0.0568	17835	6475	0.0107	0.134	0.057
72	0.08	0.0576	18086	6566	0.0109	0.136	0.058
73	0.08	0.0584	18338	6658	0.0110	0.138	0.058
74	0.08	0.0592	18589	6749	0.0112	0.139	0.059
75	0.08	0.0600	18840	6840	0.0113	0.141	0.060
76	0.08	0.0608	19091	6931	0.0115	0.143	0.061
77	0.08	0.0616	19342	7022	0.0116	0.145	0.062
78	0.08	0.0624	19594	7114	0.0118	0.147	0.062
79	0.08	0.0632	19845	7205	0.0119	0.149	0.063
80	0.08	0.0640	20096	7296	0.0121	0.151	0.064
81	0.08	0.0648	20347	7387	0.0122	0.153	0.065
82	0.08	0.0656	20598	7478	0.0124	0.154	0.066
83	0.08	0.0664	20850	7570	0.0125	0.156	0.066
84	0.08	0.0672	21101	7661	0.0127	0.158	0.067
85	0.08	0.0680	21352	7752	0.0128	0.160	0.068
86	0.08	0.0688	21603	7843	0.0130	0.162	0.069
87	0.08	0.0696	21854	7934	0.0131	0.164	0.070
88	0.08	0.0704	22106	8026	0.0133	0.166	0.070
89	0.08	0.0712	22357	8117	0.0134	0.168	0.071
90	0.08	0.0720	22608	8208	0.0136	0.170	0.072
91	0.08	0.0728	22859	8299	0.0137	0.171	0.073
92	0.08	0.0736	23110	8390	0.0139	0.173	0.074
93	0.08	0.0744	23362	8482	0.0140	0.175	0.074
94	0.08	0.0752	23613	8573	0.0142	0.177	0.075
95	0.08	0.0760	23864	8664	0.0143	0.179	0.076
96	0.08	0.0768	24115	8755	0.0145	0.181	0.077
97	0.08	0.0776	24366	8846	0.0146	0.183	0.078
98	0.08	0.0784	24618	8938	0.0148	0.185	0.078
99	0.08	0.0792	24869	9029	0.0149	0.187	0.079
100	0.08	0.0800	25120	9120	0.0151	**0.188**	0.080

Table I2. Z-200 Carriers – Displacement Ranging from 0% to 100% Fill

Percent Fill (%)	Total Water Volume (m3)	Actual Water Volume (m3)	Number of Z-200 Pieces	Mass of Z-200 Pieces (g)	Volume of Liquid Displaced (m3)	Ratio of Volume of Liquid Displaced to Total Water Volume	Volume Occupied by Z-200 (m3)
0	0.08	0.0000	0	0	0.0000	0.000	0.000
1	0.08	0.0008	483	178	0.0002	0.002	0.001
2	0.08	0.0016	966	357	0.0004	0.005	0.002
3	0.08	0.0024	1450	535	0.0006	0.007	0.002
4	0.08	0.0032	1933	714	0.0008	0.010	0.003
5	0.08	0.0040	2416	892	0.0010	0.012	0.004
6	0.08	0.0048	2899	1070	0.0012	0.014	0.005
7	0.08	0.0056	3382	1249	0.0014	0.017	0.006
8	0.08	0.0064	3866	1427	0.0015	0.019	0.006
9	0.08	0.0072	4349	1606	0.0017	0.022	0.007
10	0.08	0.0080	4832	1784	0.0019	0.024	0.008
11	0.08	0.0088	5315	1962	0.0021	0.027	0.009
12	0.08	0.0096	5798	2141	0.0023	0.029	0.010
13	0.08	0.0104	6282	2319	0.0025	0.031	0.010
14	0.08	0.0112	6765	2498	0.0027	0.034	0.011
15	0.08	0.0120	7248	2676	0.0029	0.036	0.012
16	0.08	0.0128	7731	2854	0.0031	0.039	0.013
17	0.08	0.0136	8214	3033	0.0033	0.041	0.014
18	0.08	0.0144	8698	3211	0.0035	0.043	0.014
19	0.08	0.0152	9181	3390	0.0037	0.046	0.015
20	0.08	0.0160	9664	3568	0.0039	0.048	0.016
21	0.08	0.0168	10147	3746	0.0041	0.051	0.017
22	0.08	0.0176	10630	3925	0.0043	0.053	0.018
23	0.08	0.0184	11114	4103	0.0044	0.056	0.018
24	0.08	0.0192	11597	4282	0.0046	0.058	0.019
25	0.08	0.0200	12080	4460	0.0048	0.060	0.020
26	0.08	0.0208	12563	4638	0.0050	0.063	0.021
27	0.08	0.0216	13046	4817	0.0052	0.065	0.022
28	0.08	0.0224	13530	4995	0.0054	0.068	0.022
29	0.08	0.0232	14013	5174	0.0056	0.070	0.023
30	0.08	0.0240	14496	5352	0.0058	0.072	0.024
31	0.08	0.0248	14979	5530	0.0060	0.075	0.025
32	0.08	0.0256	15462	5709	0.0062	0.077	0.026

33	0.08	0.0264	15946	5887	0.0064	0.080	0.026
34	0.08	0.0272	16429	6066	0.0066	0.082	0.027
35	0.08	0.0280	16912	6244	0.0068	0.085	0.028
36	0.08	0.0288	17395	6422	0.0070	0.087	0.029
37	0.08	0.0296	17878	6601	0.0072	0.089	0.030
38	0.08	0.0304	18362	6779	0.0073	0.092	0.030
39	0.08	0.0312	18845	6958	0.0075	0.094	0.031
40	0.08	0.0320	19328	7136	0.0077	0.097	0.032
41	0.08	0.0328	19811	7314	0.0079	0.099	0.033
42	0.08	0.0336	20294	7493	0.0081	0.101	0.034
43	0.08	0.0344	20778	7671	0.0083	0.104	0.034
44	0.08	0.0352	21261	7850	0.0085	0.106	0.035
45	0.08	0.0360	21744	8028	0.0087	0.109	0.036
46	0.08	0.0368	22227	8206	0.0089	0.111	0.037
47	0.08	0.0376	22710	8385	0.0091	0.114	0.038
48	0.08	0.0384	23194	8563	0.0093	0.116	0.038
49	0.08	0.0392	23677	8742	0.0095	0.118	0.039
50	0.08	0.0400	24160	8920	0.0097	0.121	0.040
51	0.08	0.0408	24643	9098	0.0099	0.123	0.041
52	0.08	0.0416	25126	9277	0.0101	0.126	0.042
53	0.08	0.0424	25610	9455	0.0102	0.128	0.042
54	0.08	0.0432	26093	9634	0.0104	0.130	0.043
55	0.08	0.0440	26576	9812	0.0106	0.133	0.044
56	0.08	0.0448	27059	9990	0.0108	0.135	0.045
57	0.08	0.0456	27542	10169	0.0110	0.138	0.046
58	0.08	0.0464	28026	10347	0.0112	0.140	0.046
59	0.08	0.0472	28509	10526	0.0114	0.143	0.047
60	0.08	0.0480	28992	10704	0.0116	0.145	0.048
61	0.08	0.0488	29475	10882	0.0118	0.147	0.049
62	0.08	0.0496	29958	11061	0.0120	0.150	0.050
63	0.08	0.0504	30442	11239	0.0122	0.152	0.050
64	0.08	0.0512	30925	11418	0.0124	0.155	0.051
65	0.08	0.0520	31408	11596	0.0126	0.157	0.052

66	0.08	0.0528	31891	11774	0.0128	0.159	0.053
67	0.08	0.0536	32374	11953	0.0129	0.162	0.054
68	0.08	0.0544	32858	12131	0.0131	0.164	0.054
69	0.08	0.0552	33341	12310	0.0133	0.167	0.055
70	0.08	0.0560	33824	12488	0.0135	0.169	0.056
71	0.08	0.0568	34307	12666	0.0137	0.172	0.057
72	0.08	0.0576	34790	12845	0.0139	0.174	0.058
73	0.08	0.0584	35274	13023	0.0141	0.176	0.058
74	0.08	0.0592	35757	13202	0.0143	0.179	0.059
75	0.08	0.0600	36240	13380	0.0145	0.181	0.060
76	0.08	0.0608	36723	13558	0.0147	0.184	0.061
77	0.08	0.0616	37206	13737	0.0149	0.186	0.062
78	0.08	0.0624	37690	13915	0.0151	0.188	0.062
79	0.08	0.0632	38173	14094	0.0153	0.191	0.063
80	0.08	0.0640	38656	14272	0.0155	0.193	0.064
81	0.08	0.0648	39139	14450	0.0157	0.196	0.065
82	0.08	0.0656	39622	14629	0.0158	0.198	0.066
83	0.08	0.0664	40106	14807	0.0160	0.201	0.066
84	0.08	0.0672	40589	14986	0.0162	0.203	0.067
85	0.08	0.0680	41072	15164	0.0164	0.205	0.068
86	0.08	0.0688	41555	15342	0.0166	0.208	0.069
87	0.08	0.0696	42038	15521	0.0168	0.210	0.070
88	0.08	0.0704	42522	15699	0.0170	0.213	0.070
89	0.08	0.0712	43005	15878	0.0172	0.215	0.071

90	0.08	0.0720	43488	16056	0.0174	0.217	0.072
91	0.08	0.0728	43971	16234	0.0176	0.220	0.073
92	0.08	0.0736	44454	16413	0.0178	0.222	0.074
93	0.08	0.0744	44938	16591	0.0180	0.225	0.074
94	0.08	0.0752	45421	16770	0.0182	0.227	0.075
95	0.08	0.0760	45904	16948	0.0184	0.230	0.076
96	0.08	0.0768	46387	17126	0.0186	0.232	0.077
97	0.08	0.0776	46870	17305	0.0187	0.234	0.078
98	0.08	0.0784	47354	17483	0.0189	0.237	0.078
99	0.08	0.0792	47837	17662	0.0191	0.239	0.079
100	0.08	0.0800	48320	17840	0.0193	**0.242**	0.080

Table I3. Z-200 Carriers – Displacement Ranging from 0% to 100% Fill

Percent Fill (%)	Total Water Volume (m3)	Actual Water Volume (m3)	Number of Z-200 Pieces	Mass of Z-200 Pieces (g)	Volume of Liquid Displaced (m3)	Ratio of Volume of Liquid Displaced to Total Water Volume	Volume Occupied by Z-200 (m3)
0	0.08	0.0000	0	0	0.0000	0.000	0.000
1	0.08	0.0008	491	186	0.0002	0.002	0.001
2	0.08	0.0016	982	371	0.0004	0.005	0.002
3	0.08	0.0024	1474	557	0.0006	0.007	0.002
4	0.08	0.0032	1965	742	0.0008	0.010	0.003
5	0.08	0.0040	2456	928	0.0010	0.012	0.004
6	0.08	0.0048	2947	1114	0.0012	0.015	0.005
7	0.08	0.0056	3438	1299	0.0014	0.017	0.006
8	0.08	0.0064	3930	1485	0.0016	0.020	0.006
9	0.08	0.0072	4421	1670	0.0018	0.022	0.007
10	0.08	0.0080	4912	1856	0.0020	0.025	0.008
11	0.08	0.0088	5403	2042	0.0022	0.027	0.009
12	0.08	0.0096	5894	2227	0.0024	0.029	0.010
13	0.08	0.0104	6386	2413	0.0026	0.032	0.010
14	0.08	0.0112	6877	2598	0.0028	0.034	0.011
15	0.08	0.0120	7368	2784	0.0029	0.037	0.012
16	0.08	0.0128	7859	2970	0.0031	0.039	0.013
17	0.08	0.0136	8350	3155	0.0033	0.042	0.014
18	0.08	0.0144	8842	3341	0.0035	0.044	0.014
19	0.08	0.0152	9333	3526	0.0037	0.047	0.015
20	0.08	0.0160	9824	3712	0.0039	0.049	0.016
21	0.08	0.0168	10315	3898	0.0041	0.052	0.017
22	0.08	0.0176	10806	4083	0.0043	0.054	0.018
23	0.08	0.0184	11298	4269	0.0045	0.056	0.018
24	0.08	0.0192	11789	4454	0.0047	0.059	0.019
25	0.08	0.0200	12280	4640	0.0049	0.061	0.020
26	0.08	0.0208	12771	4826	0.0051	0.064	0.021
27	0.08	0.0216	13262	5011	0.0053	0.066	0.022
28	0.08	0.0224	13754	5197	0.0055	0.069	0.022
29	0.08	0.0232	14245	5382	0.0057	0.071	0.023
30	0.08	0.0240	14736	5568	0.0059	0.074	0.024
31	0.08	0.0248	15227	5754	0.0061	0.076	0.025
32	0.08	0.0256	15718	5939	0.0063	0.079	0.026

33	0.08	0.0264	16210	6125	0.0065	0.081	0.026
34	0.08	0.0272	16701	6310	0.0067	0.084	0.027
35	0.08	0.0280	17192	6496	0.0069	0.086	0.028
36	0.08	0.0288	17683	6682	0.0071	0.088	0.029
37	0.08	0.0296	18174	6867	0.0073	0.091	0.030
38	0.08	0.0304	18666	7053	0.0075	0.093	0.030
39	0.08	0.0312	19157	7238	0.0077	0.096	0.031
40	0.08	0.0320	19648	7424	0.0079	0.098	0.032
41	0.08	0.0328	20139	7610	0.0081	0.101	0.033
42	0.08	0.0336	20630	7795	0.0083	0.103	0.034
43	0.08	0.0344	21122	7981	0.0084	0.106	0.034
44	0.08	0.0352	21613	8166	0.0086	0.108	0.035
45	0.08	0.0360	22104	8352	0.0088	0.111	0.036
46	0.08	0.0368	22595	8538	0.0090	0.113	0.037
47	0.08	0.0376	23086	8723	0.0092	0.115	0.038
48	0.08	0.0384	23578	8909	0.0094	0.118	0.038
49	0.08	0.0392	24069	9094	0.0096	0.120	0.039
50	0.08	0.0400	24560	9280	0.0098	0.123	0.040
51	0.08	0.0408	25051	9466	0.0100	0.125	0.041
52	0.08	0.0416	25542	9651	0.0102	0.128	0.042
53	0.08	0.0424	26034	9837	0.0104	0.130	0.042
54	0.08	0.0432	26525	10022	0.0106	0.133	0.043
55	0.08	0.0440	27016	10208	0.0108	0.135	0.044
56	0.08	0.0448	27507	10394	0.0110	0.138	0.045
57	0.08	0.0456	27998	10579	0.0112	0.140	0.046
58	0.08	0.0464	28490	10765	0.0114	0.142	0.046
59	0.08	0.0472	28981	10950	0.0116	0.145	0.047
60	0.08	0.0480	29472	11136	0.0118	0.147	0.048
61	0.08	0.0488	29963	11322	0.0120	0.150	0.049
62	0.08	0.0496	30454	11507	0.0122	0.152	0.050
63	0.08	0.0504	30946	11693	0.0124	0.155	0.050
64	0.08	0.0512	31437	11878	0.0126	0.157	0.051

65	0.08	0.0520	31928	12064	0.0128	0.160	0.052
66	0.08	0.0528	32419	12250	0.0130	0.162	0.053
67	0.08	0.0536	32910	12435	0.0132	0.165	0.054
68	0.08	0.0544	33402	12621	0.0134	0.167	0.054
69	0.08	0.0552	33893	12806	0.0136	0.169	0.055
70	0.08	0.0560	34384	12992	0.0138	0.172	0.056
71	0.08	0.0568	34875	13178	0.0140	0.174	0.057
72	0.08	0.0576	35366	13363	0.0141	0.177	0.058
73	0.08	0.0584	35858	13549	0.0143	0.179	0.058
74	0.08	0.0592	36349	13734	0.0145	0.182	0.059
75	0.08	0.0600	36840	13920	0.0147	0.184	0.060
76	0.08	0.0608	37331	14106	0.0149	0.187	0.061
77	0.08	0.0616	37822	14291	0.0151	0.189	0.062
78	0.08	0.0624	38314	14477	0.0153	0.192	0.062
79	0.08	0.0632	38805	14662	0.0155	0.194	0.063
80	0.08	0.0640	39296	14848	0.0157	0.196	0.064
81	0.08	0.0648	39787	15034	0.0159	0.199	0.065
82	0.08	0.0656	40278	15219	0.0161	0.201	0.066
83	0.08	0.0664	40770	15405	0.0163	0.204	0.066
84	0.08	0.0672	41261	15590	0.0165	0.206	0.067
85	0.08	0.0680	41752	15776	0.0167	0.209	0.068
86	0.08	0.0688	42243	15962	0.0169	0.211	0.069
87	0.08	0.0696	42734	16147	0.0171	0.214	0.070
88	0.08	0.0704	43226	16333	0.0173	0.216	0.070

89	0.08	0.0712	43717	16518	0.0175	0.219	0.071
90	0.08	0.0720	44208	16704	0.0177	0.221	0.072
91	0.08	0.0728	44699	16890	0.0179	0.223	0.073
92	0.08	0.0736	45190	17075	0.0181	0.226	0.074
93	0.08	0.0744	45682	17261	0.0183	0.228	0.074
94	0.08	0.0752	46173	17446	0.0185	0.231	0.075
95	0.08	0.0760	46664	17632	0.0187	0.233	0.076
96	0.08	0.0768	47155	17818	0.0189	0.236	0.077
97	0.08	0.0776	47646	18003	0.0191	0.238	0.078
98	0.08	0.0784	48138	18189	0.0193	0.241	0.078
99	0.08	0.0792	48629	18374	0.0195	0.243	0.079
100	0.08	0.0800	49120	18560	0.0196	**0.246**	0.080